Scattering

1 . Introduction

Scattering occurs whenever a wave impinges on a body. The discontinuity in impedance at the surface of the scatterer leads to the reflection/transmission of all the Huygens' wavelets incident on the scatterer. The reflections occur in all directions and it is referred to as scattering.

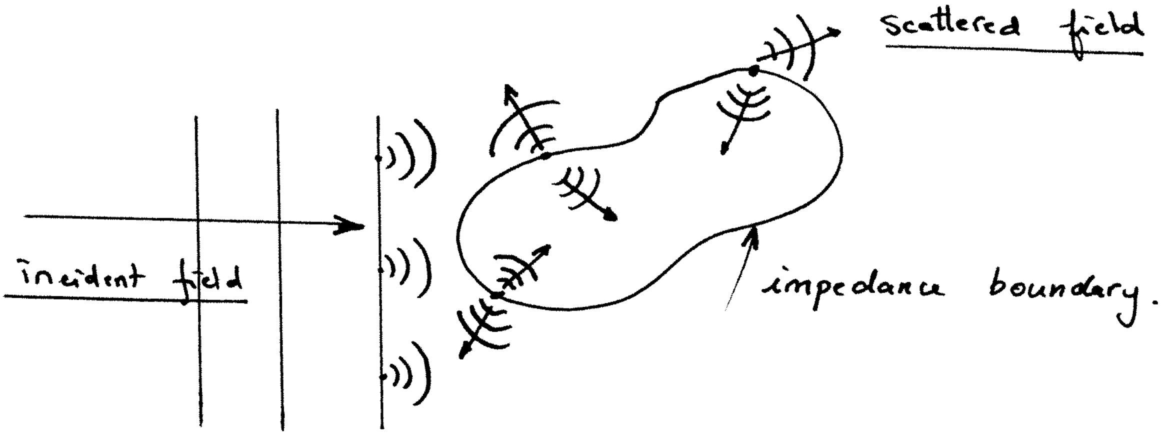

Scattering is the fundamental mechanism behind acoustical imag

Nondestructive Testing

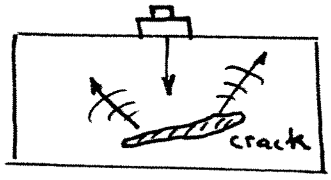

Geophysics

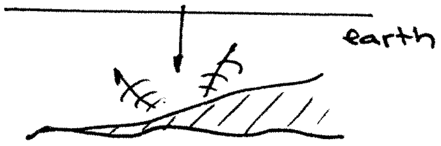

Medical Ultrasonics

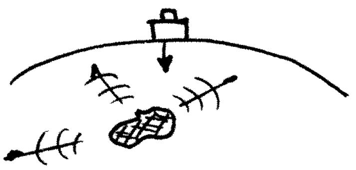

Sonar (ASW)

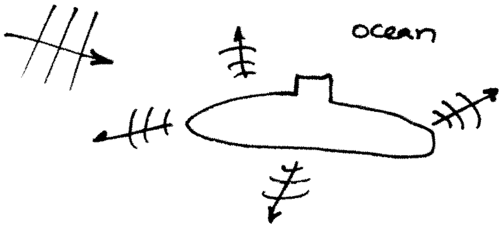

The echo from an elastic target is, in general, compos of 3 contributions :

1) - Specular reflection
2) - Elastic echo (reflection - transmission inside)
3) - Diffraction echo (creeping waves)

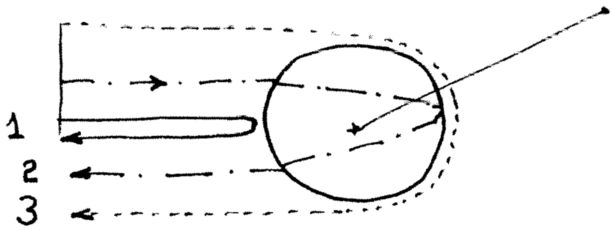

$P_s(\vec{r}) = P_T(\vec{r}) - P$

The scattered pressure at any observation point $\vec{r}$ $(r \geqslant a)$ is defined as the difference between the total pressure, P_T and the incident pressure P_i that would exist if the scatterer was not present.

$$P_s(\vec{r}) = P_T(\vec{r}) - P_i(\vec{r})$$

Most of the experimental studies are performed with transien signals. Most of the theoretical studies assume a steady state time-harmonic incident wave.

The transient and steady state harmonic solutions are related by :

$$P_s(r,\theta,\phi,t) = \int_{-\infty}^{+\infty} \hat{P}_s(r,\theta,\phi,\omega)\, e^{j\omega t}\, d\omega$$

or

$$\hat{P}_s(r,\theta,\phi,\omega) = \frac{1}{2\pi}\int_{-\infty}^{+\infty} P_s(r,\theta,\phi,t)\, e^{-j\omega t}\, dt$$

Scattering approaches

[See Kino, Acoustic Waves, Prentice Hall, 1987. pp. 303 - 313].
Here we list results. We will derive eqns later.

① Surface integral: (H-K integral) (Green's th)

ρ = density
κ = compressibility = ρc^2.
($Z = \sqrt{\rho \kappa}$)

[re note =

Surface of scatterer: S'

scatt. pot:

$$\boxed{\phi_s = \int_{S'} (\phi \nabla G - G \nabla \phi) \cdot \vec{n} \, dS'} \qquad (1)$$

$$G = \frac{e^{-jkR}}{4\pi R}$$

pb: need to know ϕ on the surface.
($\phi_T = \phi_i + \phi_s$)

② Volume integration (Gauss' theorem

Express (1) as a volume integral using Gauss' theorem

$$\boxed{P_s = \int_{V'} \left[\left(1 - \frac{\rho}{\rho'}\right) \nabla p \cdot \nabla G - k^2 p \, G \left(1 - \frac{\kappa}{\kappa'}\right) \right] dV'} \quad ($$

~~$k^2 = \omega^2 \frac{\rho}{\kappa}$~~

($P_T = P_i + P_s$)

V' = volume of scatterer.

P, G, ∇G, ∇p evaluated inside V'

Usually p not known inside scatterer $\Rightarrow$ need approximation to evaluate (2).

(a) Born approximation

p inside scatterer $\simeq$ p incident . (!)

$\Longleftrightarrow$ small contrast in ρ, κ between inside/outsid
(Z)

if, in addition, $\lambda \gg a$ → low ka →
" Rayleigh approximati

Then

$$\boxed{\frac{P_s}{P_i} = -k^2 V \left[\frac{e^{j(\omega t - kr)}}{r}\right]\left[\left(1-\frac{\kappa}{\kappa'}\right)+\left(\frac{\rho}{\rho'}-1\right)\cos\theta\right]}$$

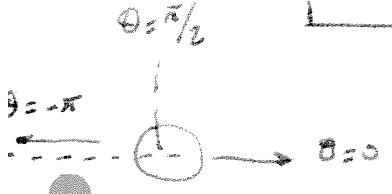

higher frequencies are more scattered than lower frequencies.

compressibility (monopole)

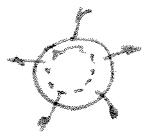

inertia (dipole

(b) Quasi-static approximation.

If contrast in ρ, κ very high
still low ka, Rayleigh approximation.

Assume that, near the object $\nabla^2 p \gg k^2 p$

large gradient

low frequency

large gradient ∇p near the object.

(so $\nabla^2 p = 0$)

Then $$\boxed{\frac{P_s}{P_I} = -k^2 V \left[\frac{e^{j(\omega t - kr)}}{4\pi r}\right]\left\{\left(1-\frac{\kappa'}{\kappa}\right) + \cos\theta \cdot \frac{1-\frac{\rho'}{\rho}}{1+2\frac{\rho'}{\rho}}\right.}$$

Monopole (compressibility)

dipole (inertia

Now we derive general expressions for P_s for both rigid and elastic scatterers.

method: modal expansion.

Rayleigh's dimensional analysis. Theory of Sound, Dover, Vol.2, p153.

$P_s(r)$ must depend on $\lambda, V, r,$

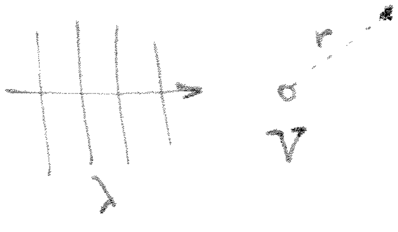

$$\frac{P_s}{P_{inc}} = \frac{V}{r}\lambda^m$$ find m.

for dimensional compatibility $m = -2$ $$\Longrightarrow \boxed{\frac{P_s}{P_{inc}} = \frac{V}{r\lambda^2}} = \frac{V}{r} f^2$$

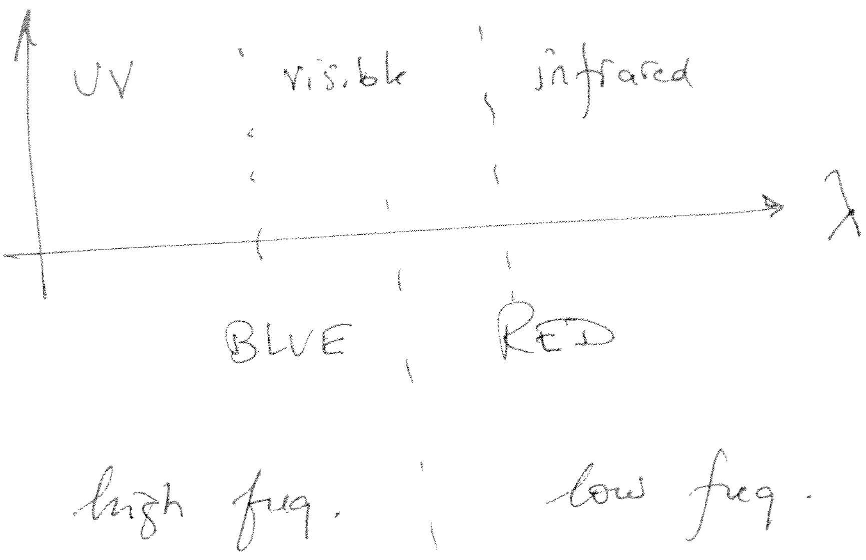

Blue is more scattered than red

→ sky is blue. Blue

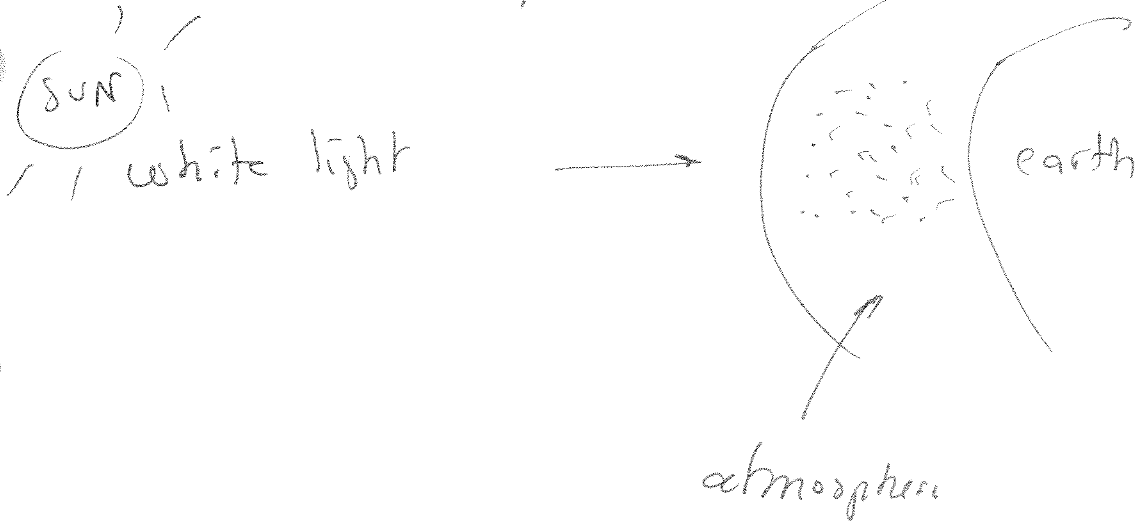

on earth we receive only scattered light → Blue

THE

THEORY OF SOUND

BY

JOHN WILLIAM STRUTT, BARON RAYLEIGH, Sc.D., F.R.S.
HONORARY FELLOW OF TRINITY COLLEGE, CAMBRIDGE

WITH A HISTORICAL INTRODUCTION BY
ROBERT BRUCE LINDSAY
HAZARD PROFESSOR OF PHYSICS IN BROWN UNIVERSITY

IN TWO VOLUMES

VOLUME II
SECOND EDITION REVISED AND ENLARGED

NEW YORK
DOVER PUBLICATIONS

so that
$$\frac{dT}{dt} = \rho_0 \iiint \Sigma \frac{d\phi}{dx}\frac{d\dot{\phi}}{dx}\,dV$$
$$= \rho_0 \iint \dot{\phi}\frac{d\phi}{dn}\,dS - \rho_0 \iiint \dot{\phi}\,\nabla^2\phi\,dV \quad\ldots\ldots\ldots\ldots\ldots\ldots (2),$$

by Green's theorem. For the potential energy V_1 we have by (12) § 245

$$V_1 = \frac{\rho_0}{2a^2}\iiint \phi^2 dV \quad\ldots\ldots\ldots\ldots\ldots\ldots\ldots\ldots (3),$$

whence
$$\frac{dV_1}{dt} = \frac{\rho_0}{a^2}\iiint \dot{\phi}\ddot{\phi}\,dV = \frac{\rho_0}{a^2}\iiint \left\{\frac{dR}{dt} + a^2\nabla^2\phi\right\}\dot{\phi}\,dV \ldots (4),$$

by the general equation of motion (9) § 244. Thus, if E denote the whole energy within the space S,

$$\frac{dE}{dt} = \rho_0 \iint \dot{\phi}\frac{d\phi}{dn}\,dS + \frac{\rho_0}{a^2}\iiint \frac{dR}{dt}\,\dot{\phi}\,dV \quad\ldots\ldots\ldots\ldots (5),$$

of which the first term represents the work transmitted across the boundary S, and the second represents the work done by internal sources of sound.

If the boundary S be a fixed rigid envelope, and there be no internal sources, E retains its initial value throughout the motion. This principle has been applied by Kirchhoff[1] to prove the determinateness of the motion resulting from given arbitrary initial conditions. Since every element of E is positive, there can be no motion within S, if E be zero. Now, if there were two motions possible corresponding to the same initial conditions, their difference would be a motion for which the initial value of E was zero; but by what has just been said such a motion cannot exist.

---

[1] *Vorlesungen über Math. Physik*, p. 311.

CHAPTER XV.

FURTHER APPLICATION OF THE GENERAL EQUATIONS.

296. WHEN a train of plane waves, otherwise unimpeded, impinges upon a space occupied by matter, whose mechanical properties differ from those of the surrounding medium, secondary waves are thrown off, which may be regarded as a disturbance due to the change in the nature of the medium—a point of view more especially appropriate, when the *region of disturbance*, as well as the alteration of mechanical properties, is small. If the medium and the obstacle be fluid, the mechanical properties spoken of are two—the *compressibility* and the *density*: no account is here taken of friction or viscosity. In the chapter on spherical harmonic analysis we shall consider the problem here proposed on the supposition that the obstacle is spherical, without any restriction as to the smallness of the change of mechanical properties; in the present investigation the form of the obstacle is arbitrary, but we assume that the squares and higher powers of the changes of mechanical properties may be omitted.

If ξ, η, ζ denote the displacements parallel to the axes of co-ordinates of the particle, whose equilibrium position is defined by x, y, z, and if σ be the normal density, and m the constant of compressibility so that $\delta p = ms$, the equations of motion are

$$\sigma\frac{d^2\xi}{dt^2} + \frac{d\,(ms)}{dx} = 0 \quad\ldots\ldots\ldots\ldots\ldots\ldots\ldots (1),$$

and two similar equations in η and ζ. On the assumption that the whole motion is proportional to e^{ikat}, where as usual $k = 2\pi/\lambda$, and (§ 244) $a^2 = m/\sigma$, (1) may be written

$$\frac{d\,(ms)}{dx} - \sigma k^2 a^2 \xi = 0 \quad\ldots\ldots\ldots\ldots\ldots\ldots\ldots (2).$$

The relation between the condensation s, and the displacements ξ, η, ζ, obtained by integrating (3) § 238 with respect to the time, is

$$-s = \frac{d\xi}{dx} + \frac{d\eta}{dy} + \frac{d\zeta}{dz} \quad\text{.....................}(3).$$

For the system of primary waves advancing in the direction of $-x$, η and ζ vanish; if ξ_0, s_0 be the values of ξ and s, and m_0, σ_0 be the mechanical constants for the undisturbed medium, we have as in (2)

$$\frac{d\,(m_0 s_0)}{dx} - \sigma_0 k^2 a^2 \xi_0 = 0 \quad\text{.................}(4);$$

but ξ_0, s_0 do not satisfy (2) at the region of disturbance on account of the variation in m and σ, which occurs there. Let us assume that the complete values are $\xi_0 + \xi$, η, ζ, $s_0 + s$ [1], and substitute in (2). Then taking account of (4), we get

$$\frac{d\,(ms)}{dx} - \sigma k^2 a^2 \xi + (m - m_0)\frac{ds_0}{dx} + s_0 \frac{dm}{dx} - (\sigma - \sigma_0)\, k^2 a^2 \xi_0 = 0,$$

or, as it may also be written,

$$\frac{d}{dx}(ms) - \sigma k^2 a^2 \xi + \frac{d}{dx}(\Delta m . s_0) - \Delta\sigma . k^2 a^2 \xi_0 = 0 \quad\text{......}\ (5),$$

if Δm, $\Delta\sigma$ stand respectively for $m - m_0$, $\sigma - \sigma_0$. The equations in η and ζ are in like manner

$$\left.\begin{aligned} \frac{d}{dy}(ms) - \sigma k^2 a^2 \eta + \frac{d}{dy}(\Delta m . s_0) &= 0 \\ \frac{d}{dz}(ms) - \sigma k^2 a^2 \zeta + \frac{d}{dz}(\Delta m . s_0) &= 0, \end{aligned}\right\} \quad\text{.........}\ (6).$$

It is to be observed that Δm, $\Delta\sigma$ vanish, except through a small space, which is regarded as the region of disturbance; ξ, η, ζ, s, being the result of the disturbance are to be treated as small quantities of the order Δm, $\Delta\sigma$; so that in our approximate analysis the variations of m and σ in the first two terms of (5) and (6) are to be neglected, being there multiplied by small quantities. We thus obtain from (5) and (6) by differentiation and addition, with use of (3), as the differential equation in s,

$$\nabla^2 (ms) + k^2 ms = k^2 a^2 \frac{d}{dx}(\Delta\sigma . \xi_0) - \nabla^2 (\Delta m . s_0) \quad\text{......}(7).$$

---

[1] [This notation was adopted for brevity. It might be clearer to take $\xi = \xi_0 + \Delta\xi$, $s = s_0 + \Delta s$, &c.; so that ξ, s, &c. should retain their former meanings.]

As in § 277, the solution of (7) is

$$4\pi m\, s = \iiint \frac{e^{-ikr}}{r} \left\{ \nabla^2 (\Delta m . s_0) - k^2 a^2 \frac{d}{dx}(\Delta\sigma . \xi_0) \right\} dV \text{......}(8),$$

in which the integration extends over a volume completely including the region of disturbance. The integrals in (8) may be transformed with the aid of Green's theorem. Calling the two parts respectively P and Q, we have

$$P = \iiint \frac{e^{-ikr}}{r} \nabla^2 (\Delta m . s_0)\, dV = \iiint \Delta m . s_0 \nabla^2 \left(\frac{e^{-ikr}}{r}\right) dV$$

$$+ \iint \left\{ \frac{e^{-ikr}}{r} \frac{d}{dn}(\Delta m . s_0) - \Delta m . s_0 \frac{d}{dn}\left(\frac{e^{-ikr}}{r}\right) \right\} dS,$$

where S denotes the surface of the space through which the triple integration extends. Now on S, Δm and $\frac{d}{dn}(\Delta m . s_0)$ vanish, so that both the surface integrals disappear. Moreover

$$\nabla^2 \left(\frac{e^{-ikr}}{r}\right) = \frac{1}{r}\frac{d^2}{dr^2} e^{-ikr} = -k^2 \frac{e^{-ikr}}{r};$$

and thus

$$P = -k^2 \iiint \frac{e^{-ikr}}{r} \Delta m . s_0\, dV \quad\text{.................}(9).$$

If the region of disturbance be small in comparison with λ, we may write

$$P = -k^2 s_0 \frac{e^{-ikr}}{r} \iiint \Delta m dV \quad\text{.................}(10).$$

In like manner for the second integral in (8), we find

$$Q = -k^2 a^2 \iiint \frac{e^{-ikr}}{r} \frac{d}{dx}(\Delta\sigma . \xi_0)\, dV$$

$$= k^2 a^2 \iiint \Delta\sigma . \xi_0 \frac{d}{dx}\left(\frac{e^{-ikr}}{r}\right) dV = ik^3 a^2 \xi_0 \mu \frac{e^{-ikr}}{r} \iiint \Delta\sigma dV \text{...}(11),$$

where μ denotes the cosine of the angle between x and r. The linear dimension of the region of disturbance is neglected in comparison with λ, and λ is neglected in comparison with r.

If T be the volume of the space through which Δm, $\Delta\sigma$ are sensible, we may write

$$\iiint \Delta m\, dV = T . \Delta m, \qquad \iiint \Delta\sigma\, dV = T . \Delta\sigma,$$

if on the right-hand sides Δm, $\Delta\sigma$ refer to the *mean values* of the variations in question. Thus from (8)

$$s = -\frac{k^2 T e^{-ikr}}{4\pi m\, r}\left\{\Delta m . s_0 - ika^2 \Delta\sigma . \xi_0\, \mu\right\} \text{ ......(12).}$$

To express ξ_0 in terms of s_0, we have from (3), $\xi_0 = -\int s_0\, dx$; and thus, if the condensation for the primary waves be $s_0 = e^{ik(at+x)}$, $ik\xi_0 = -s_0$, and (12) may be put into the form

$$s : s_0 = -\frac{\pi T e^{-ikr}}{\lambda^2 r}\left\{\frac{\Delta m}{m} + \frac{\Delta\sigma}{\sigma}\mu\right\} \text{ ....(13),}$$

in which s_0 denotes the condensation of the primary waves at the place of disturbance at time t, and s denotes the condensation of the secondary waves at the same time at a distance r from the disturbance. Since the difference of phase represented by the factor e^{-ikr} corresponds simply to the distance r, we may consider that a simple reversal of phase occurs at the place of disturbance. The amplitude of the secondary waves is inversely proportional to the distance r, and to the *square* of the wave-length λ. Of the two terms expressed in (13) the first is symmetrical in all directions round the place of disturbance, while the second varies as the cosine of the angle between the primary and the secondary rays. Thus a place at which m varies behaves as a *simple* source, and a place at which σ varies behaves as a *double* source (§ 294).

That the secondary disturbance must vary as λ^{-2} may be proved immediately by the method of dimensions. Δm and $\Delta\sigma$ being given, the amplitude is necessarily proportional to T, and in accordance with the principle of energy must also vary inversely as r. Now the only quantities (dependent upon space, time, and mass) of which the ratio of amplitudes can be a function, are T, r, λ, a (the velocity of sound), and σ, of which the last cannot occur in the expression of a simple ratio, as it is the only one of the five which involves a reference to mass. Of the remaining four quantities T, r, λ, and a, the last is the only one which involves a reference to time, and is therefore excluded. We are left with T, r, and λ, of which the only combination varying as Tr^{-1}, and independent of the unit of length, is $Tr^{-1}\lambda^{-2}$.[1]

An interesting application of the results of this section may be made to explain what have been called *harmonic echoes*[2].

If the primary sound be a compound musical note, the various component tones are scattered in unlike proportions. The octave, for example, is sixteen times stronger relatively to the fundamental tone in the secondary than it was in the primary sound. There is thus no difficulty in understanding how it may happen that echoes returned from such reflecting bodies as groups of trees may be raised an octave. The phenomenon has also a complementary side. If a number of small bodies lie in the path of waves of sound, the vibrations which issue from them in all directions are at the expense of the energy of the main stream, and where the sound is compound, the exaltation of the higher harmonics in the scattered waves involves a proportional deficiency of them in the direct wave after passing the obstacles. This is perhaps the explanation of certain echoes which are said to return a sound graver than the original; for it is known that the pitch of a pure tone is apt to be estimated too low. But the evidence is conflicting, and the whole subject requires further careful experimental investigation; it may be commended to the attention of those who may have the necessary opportunities. While an alteration in the *character* of a sound is easily intelligible, and must indeed generally happen to a limited extent, a change in the pitch of a simple tone would be a violation of the law of forced vibrations, and hardly to be reconciled with theoretical ideas.

In obtaining (13) we have neglected the effect of the variable nature of the medium *on the disturbance*. When the disturbance on this supposition is thoroughly known, we might approximate again in the same manner. The additional terms so obtained would be necessarily of the second order in Δm, $\Delta\sigma$, so that our expressions are in all cases correct as far as the first powers of those quantities.

Even when the region of disturbance is not small in comparison with λ, the same method is applicable, provided the squares of Δm, $\Delta\sigma$ be really negligible. The total effect of any obstacle may then be calculated by integration from those of its parts. In this way we may trace the transition from a small region of disturbance whose *surface* does not come into consideration, to a thin plate of a few or of a great many square wave-lengths in area, which will ultimately reflect according to the regular optical law. But if the obstacle be at all elongated in the direction of the primary rays, this method of calculation soon

---

[1] "On the Light from the Sky," *Phil. Mag.* Feb. 1871, and "On the scattering of Light by small Particles," *Phil. Mag.* June, 1871.

[2] *Nature*, 1873, VIII. 319.

ceases to be practically available, because, even although the change of mechanical properties be very small, the interaction of the various parts of the obstacle cannot be left out of account. This caution is more especially needed in dealing with the case of light, where the wave-length is so exceedingly small in comparison with the dimensions of ordinary obstacles.

297. In some degree similar to the effect produced by a change in the mechanical properties of a small region of the fluid, is that which ensues when the square of the motion rises anywhere to such importance that it can be no longer neglected. $\nabla^2\phi + k^2\phi$ then acquires a finite value dependent upon the square of the motion. Such places therefore act like sources of sound; the periods of the sources including the submultiples of the original period. Thus any part of space, at which the intensity accumulates to a sufficient extent, becomes itself a secondary source, emitting the harmonic tones of the primary sound. If there be two primary sounds of sufficient intensity, the secondary vibrations have frequencies which are the sums and differences of the frequencies of the primaries (§ 68)[1].

298. The pitch of a sound is liable to modification when the source and the recipient are in relative motion. It is clear, for instance, that an observer approaching a fixed source will meet the waves with a frequency exceeding that proper to the sound, by the number of wave-lengths passed over in a second of time. Thus if v be the velocity of the observer and a that of sound, the frequency is altered in the ratio $a \pm v : a$, according as the motion is towards or from the source. Since the alteration of pitch is constant, a musical performance would still be heard in tune, although in the second case, when a and v are nearly equal, the fall in pitch would be so great as to destroy all musical character. If we could suppose v to be greater than a, a sound produced after the motion had begun would never reach the observer, but sounds previously excited would be gradually overtaken and heard in the reverse of the natural order. If $v = 2a$, the observer would hear a musical piece in correct time and tune, but *backwards*.

Corresponding results ensue when the source is in motion and the observer at rest; the alteration depending only on the relative motion in the line of hearing. If the source and the observer move with the same velocity there is no alteration of frequency, whether

---

[1] Helmholtz über Combinationstöne. Pogg. *Ann.* Bd. XCIX. s. 497. 1856.

the medium be in motion, or not. With a relative motion of 40 miles [64 kilometres] per hour the alteration of pitch is very conspicuous, amounting to about a semitone. The whistle of a locomotive is heard too high as it approaches, and too low as it recedes from an observer at a station, changing rather suddenly at the moment of passage.

The principle of the alteration of pitch by relative motion was first enunciated by Doppler[1], and is often called Doppler's principle. Strangely enough its legitimacy was disputed by Petzval[2], whose objection was the result of a confusion between two perfectly distinct cases, that in which there is a relative motion of the source and recipient, and that in which the medium is in motion while the source and the recipient are at rest. In the latter case the circumstances are mechanically the same as if the medium were at rest and the source and the recipient had a common motion, and therefore by Doppler's principle no change of pitch is to be expected.

Doppler's principle has been experimentally verified by Buijs Ballot[3] and Scott Russell, who examined the alterations of pitch of musical instruments carried on locomotives. A laboratory instrument for proving the change of pitch due to motion has been invented by Mach[4]. It consists of a tube six feet [183 cm.] in length, capable of turning about an axis at its centre. At one end is placed a small whistle or reed, which is blown by wind forced along the axis of the tube. An observer situated in the plane of rotation hears a note of fluctuating pitch, but if he places himself in the prolongation of the axis of rotation, the sound becomes steady. Perhaps the simplest experiment is that described by König[5]. Two c'' tuning-forks mounted on resonance cases are prepared to give with each other four beats per second. If the graver of the forks be made to approach the ear while the other remains at rest, one beat is *lost* for each two feet [61 cm.] of approach; if, however, it be the more acute of the two forks which approaches the ear, one beat is *gained* in the same distance.

[illegible]

---

[1] Theorie des farbigen Lichtes der Doppelsterne. Prag, 1842. See Pisko, *Die neueren Apparate der Akustik.* Wien, 1865.

[2] *Wien. Ber.* VIII. 134. 1852. *Fortschritte der Physik*, VIII. 167.

[3] Pogg. *Ann.* LXVI. p. 321.

[4] Pogg. *Ann.* CXII. p. 66, 1861, and CXVI. p. 333, 1862.

[5] König's *Catalogue des Appareils d'Acoustique.* Paris, 1865.

2 - Scattering by a rigid sphere

2-1: Modal expansion of the incident pressure

Consider a time-harmonic plane wave, $P_i = P_o\, e^{j(\omega t - k}$ incident on a rigid sphere of radius a.

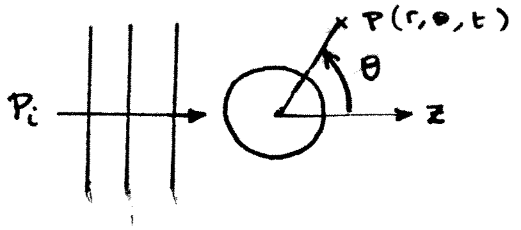

The "trick" is to expand the incident wave in terms of the eigen functions of the scatterer's geometry. Thi allows one to express in a single coordinate system th boundary conditions at $r = a$, the incident field, and the scattered field.

In spherical coordinates, any harmonic sound field that is symmetric about the z-axis (no ψ dependenc can be expressed as:

$$p(r,\theta,t) = \sum_{n=0}^{\infty} a_n\, F_n(kr)\, P_n(\cos\theta)\, e^{j\omega t}$$

where

$$F_n(kr) = \begin{Bmatrix} j_n(kr) \\ n_n(kr) \end{Bmatrix} \quad \text{or} \quad \begin{Bmatrix} h_n^{(1)}(kr) \\ h_n^{(2)}(kr) \end{Bmatrix}$$

It turns out that the choice of (j_n, n_n) is more appropriate to describe the incident sound field and that the choice of $(h_n^{(1)}, h_n^{(2)})$ is more appropriate to describe the scattered field. In addition, we discard the Neumann solution, n_n, because we want the method to be general enough to describe also scattering by an elastic sphere, in which case there would be a finite sound field inside the sphere, everywhere even at $r=0$ We also discard the $h^{(1)}(kr)$ solution for the scattered field since it represents incoming waves of the form e^{jkr}. which violate Sommerfeld's radiation condition at $r \to \infty$. The incident and scattered pressure are:

(1) $$P_i = P_0 \, e^{j(\omega t - kz)} = P_0 \sum_{n=0}^{\infty} a_n \, j_n(kr) \, P_n(\cos\theta) \, e^{j\omega}$$

(2) $$P_s = \sum_{n=0}^{\infty} b_n \, h_n^{(2)}(kr) \, P_n(\cos\theta) \, e^{j\omega t}$$

Using the orthogonality of the Legendre Polynomials in (1) it can be shown that

(3) $$a_n = (-j)^n (2n+1)$$

The proof is not trivial and it is given in the appendix. The problem at hand is thus to find the coefficient b_n in eq.(3).

2.2. Scattered pressure

The boundary condition for a rigid sphere is

(4) $$\left[\frac{\partial p}{\partial r}\right]_{r=a} = 0 \quad , \quad p = p_i + p_s = \text{total acoustic f}$$

Combining (1), (2) into (4) yields:

(5) $$P_o \sum_n k\, a_n\, j_n'(ka)\, P_n(\cos\theta) \; + \; \sum_n k\, b_n\, h_n'^{(2)}(ka)\, P_n(\cos\theta) = 0$$

The Legendre polynomials are orthogonal. Therefore (5) must be satisfied at each order n separately. To prove thi multiply both terms by $\sin\theta\, P_m(\cos\theta)$ and integrate from 0 to π. The integral

(6) $$\int_0^{\pi} P_n(\cos\theta)\, P_m(\cos\theta)\, \sin\theta\, d\theta = \int_{-1}^{1} P_m(x)\, P_n(x)\, dx = \begin{cases} 0 & \text{if } m \neq n \\ \frac{2}{2n+1} & \text{if } m = \end{cases}$$

Therefore (5) yields: $P_o\, a_n\, j_n'(ka)\, P_n(\cos\theta) + b_n\, h_n'^{(2)}(ka)\, P_n(\cos\theta) =$

or, finally, $\quad b_n = - P_o\, a_n \dfrac{j_n'(ka)}{h_n'^{(2)}(ka)} \quad ; \qquad$ with $a_n = (-j)^n (2$

The scattered pressure is, from eq. (2):

7) $$\boxed{p_s(r,\theta,t) = - P_o \sum_{n=0}^{\infty} (-j)^n (2n+1) \left[\frac{j_n'(ka)}{h_n'^{(2)}(ka)}\right] h_n^{(2)}(kr)\, P_n(\cos\theta)\, e^{j\omega}}$$

2-3 : Farfield approximation.

The farfied approximation of (7) is found by taking the asymptotic limit of $h_n^{(2)}(kr)$ for large kr.

$$\lim_{kr\to\infty} h_n^{(2)}(kr) = \lim_{kr\to\infty} \sqrt{\frac{\pi}{2kr}}\; H^{(2)}_{n+1/2}(kr)$$

§ 10.1.1
[Ab + St. p437

But $$\lim_{kr\to\infty} H_\nu^{(2)}(kr) = \sqrt{\frac{2}{\pi kr}}\; e^{-j\left(kr - \frac{\nu\pi}{2} - \frac{\pi}{4}\right)}$$

§ 9.2.4
[A+S., p36

so $$\lim_{kr\to\infty} h_n^{(2)}(kr) = \frac{1}{kr}\, e^{-j\left[kr - (n+1)\pi/2\right]}$$

so $$P_s = -P_o \left[\frac{e^{j(\omega t - kr)}}{kr}\right] \sum_{n=0}^{\infty} (-j)^n (2n+1) \left[\frac{j_n'(ka)}{h_n'^{(2)}(ka)}\right] e^{j(n+1)\pi/2}\; P_n(\cos$$

But $$e^{j\left(\frac{n+1}{2}\right)\pi} = \left(e^{j\pi/2}\right)^{n+1} = (j)^{n+1}$$

and, since $$(-j)^n (j)^{n+1} = j$$

$$\boxed{P_s = -j\, P_o \underbrace{\left[\frac{e^{j(\omega t - kr)}}{kr}\right]}_{\text{spherically spreading outward propagating wave.}} \underbrace{\sum_{n=0}^{\infty} (2n+1) \left[\frac{j_n'(ka)}{h_n'(ka)}\right] P_n(\cos\theta}_{\text{Complex amplitude directivity.}}}$$

2-4. Low-ka approximation : Rayleigh scattering

In the low-ka approximation, the b_n coefficient are :

(9) $$b_n = \lim_{ka\to 0} -P_0 \, (-j)^n \, (2n+1) \left[\frac{j'_n(ka)}{h'^{(2)}_n(ka)} \right]$$

To evaluate the bracket, we use Ref. 1 [Abramowitz an Stegun, § 10.1.4 and 10.1.5 p 437]

$$\lim_{ka\to 0} j_n(ka) = \frac{(ka)^n}{1\cdot 3\cdot 5 \cdots (2n+1)} \quad \text{and} \quad \lim_{ka\to 0} n_n(ka) = -1.3.5\ldots(ka)^{-}$$

so that $$\lim_{ka\to 0} h^{(2)}_n(ka) = \lim_{ka\to 0} \left[j_n(ka) - j\, n_n(ka) \right] = \lim_{ka\to 0} -j\, n_n(ka)$$

To obtain the low-ka approximation for the derivatives, we use the recurrence relations § 10.1.20 p 439 in Ref. 1 :

(10) $$\left\{ \begin{aligned} j'_n(ka) &= \frac{1}{2n+1} \left[n\, j_{n-1}(ka) - (n+1)\, j_{n+1}(ka) \right] \\ h'_n(ka) &= \frac{1}{2n+1} \left[n\, h_{n-1}(ka) - (n+1)\, h_{n+1}(ka) \right] \end{aligned} \right.$$

For convenience we drop the (2) index on the spherical Hankel function in the remainder of this chapter. From eq (10) it follows that :

$$\left| \begin{aligned} j'_0(ka) &= -j_1(ka) && \longrightarrow -\tfrac{1}{3}(ka) && \text{(when } ka\to 0) \\ j'_1(ka) &= \tfrac{1}{3}\left[j_0(ka) - 2 j_2(ka) \right] && \longrightarrow 1/3 \\ j'_2(ka) &= \tfrac{1}{5}\left[2 j_1 - 3 j_3 \right] && \longrightarrow \tfrac{2}{15}(ka) \\ j'_3(ka) &= \tfrac{1}{7}\left[3 j_2 - 4 j_4 \right] && \longrightarrow \tfrac{1}{35}(ka)^2 \\ j'_n(ka) &= \cdots && \longrightarrow \propto (ka)^{n-1} && n \geq 1 \end{aligned} \right.$$

Similarly

$$\left|\begin{array}{llll} h_0' = -h_1 & \longrightarrow & j\, n_1(ka) = \dfrac{-j}{(ka)^2} & \\ h_1' = \frac{1}{3}\left[h_0 - 2h_2\right] & \longrightarrow & \dfrac{-2j}{(ka)^3} & \\ h_n' = \cdots & \longrightarrow & O\left[(ka)^{-(n+2)}\right] & (n \geq 1) \end{array}\right.$$

Therefore, in the low ka limit,

$$\frac{j_0'(ka)}{h_0'(ka)} = \frac{1}{3j}(ka)^3 \qquad \text{and} \qquad \frac{j_1(ka)}{h_1'(ka)} = -\frac{1}{6j}(ka)^3$$

and, for all order $n > 2$, that ratio is of order $(ka)^{2n+}$
It follows that, at low ka, only the b_0 and b_1 coefficients are needed in the summation for the scattered pressure in eq. (8):

(11) $$P_s = -j\, P_o \left[\frac{e^{j(\omega t - kr)}}{kr}\right]\left\{\frac{1}{3j}(ka)^3 + 3\left(\frac{-1}{6j}\right)(ka)^3\cos\theta + O[(ka)\right.$$

or

(12) $$\boxed{P_s = \underbrace{P_o\left(\frac{a}{r}\right)e^{j(\omega t - kr)}}_{\text{spherical wave}}\ \underset{\substack{\downarrow \\ \text{Scattering} \\ \text{strength}}}{(ka)^2}\ \underbrace{\left[\frac{1}{2}\cos\theta - \frac{1}{3}\right]}_{\text{directivity}}}$$

$\underline{P_s \propto (ka)^2 \propto f^2}$. This is called <u>Rayleigh Scattering</u>
(low ka)

Physical interpretation:

The first term ($n=0$) in the summation has no directio
associated with it. It represents a "monopole" term. At low frequencies, the scatterer looks very small and scattering (for the $n=0$ term) occurs equally in all directions:

$n=0$, monopole term

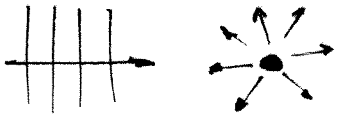

The second term ($n=1$) has a $\cos\theta$ directionality assoc
with it. It represents a "dipole" term associated wi
the transverse motion of the scatterer relative to the sound field.

$n=1$, dipole term

The Rayleigh scattering equation (12) can be used to explain why the sky is blue. As a parallel between optics and acoustics, we may use eq (12) to describe scattering of light by microscopic dust particles present in the atmosphere. In the Rayleigh scattering regime, eq. (12) shows that higher frequencies are more scattered than lower frequencies. In other words, shorter wavelengths are more easily scattered than longer wavelengths. In other words, the spectrum is shifted towards the blue and not the red.

2.5. Form function and Scattered intensity.

To display the directionality and the frequency dependence of the scattered field, it is common to introduce the farfield scattering form function $f(\theta, ka)$.

(13) $$f(\theta, ka) = \frac{|P_s(r, \theta, ka)|}{\frac{P_0}{2}\left(\frac{a}{r}\right)}$$

From eq (8), it follows that

(14) $$\boxed{f(\theta, ka) = \left(\frac{2}{ka}\right)\left|\sum_{n=0}^{\infty}(2n+1)\left[\frac{j_n'(ka)}{h_n'(ka)}\right]P_n(\cos\theta)\right|}$$

The form function can be understood as representing th interference level, in the farfield, between the ~~Scattered~~ diffracted field (wave theory) and the specular reflection (ray theory). This will be discussed in more detail in section 2.6.

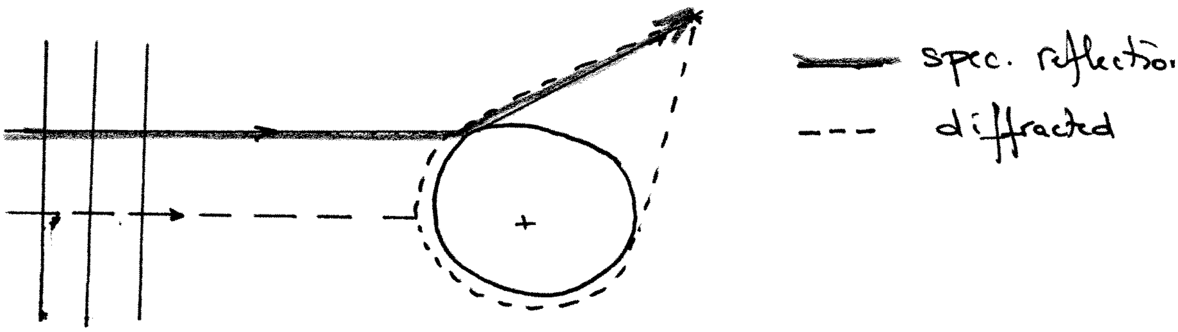


shedding from creeping waves (Franz waves

See Pierce p. 475

Low ka - approximation : From eq. (12) it follows that :

$$(15) \qquad f(\theta, ka) = \frac{P_0\left(\frac{a}{r}\right)(ka)^2\left(\frac{1}{3}-\frac{1}{2}\cos\theta\right)}{\left(\frac{P_0}{2}\right)\left(\frac{a}{r}\right)} = \underline{\underline{(ka)^2\left(\frac{2}{3}-\cos\right.}}$$

The acoustic intensity of the scattered sound is given by :

$$\vec{I}_{s,av} = \frac{1}{2}\,Re\left(\hat{p}^{*}\,\hat{\vec{U}}_s\right) \qquad \text{(See Pierce p.39}$$

where , av , refers to time average ; Re denotes the real part , and the "hat" stands for complex amplitude It can be shown that , in the farfield ,

$$(16) \qquad \boxed{\vec{I}_{s,av} = \frac{1}{2\rho c}\left|\hat{P}_s(r,\theta,ka)\right|^2 \vec{e_r}}$$

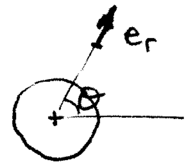

Therefore we can plot the scattered intensity directivities for various ka :

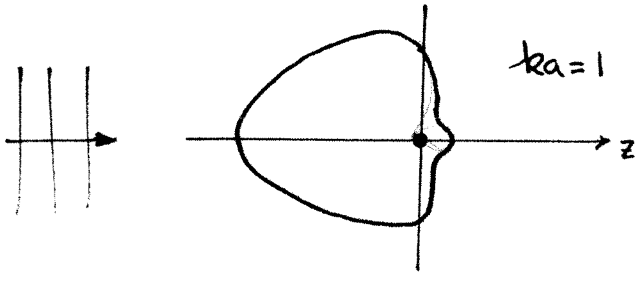

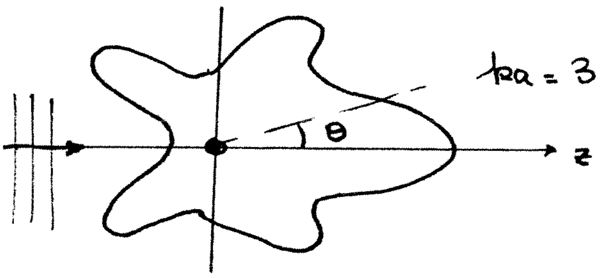

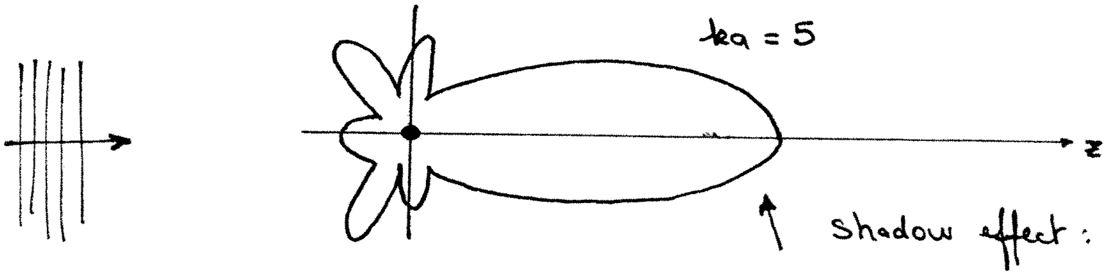

shadow effect : P_s large $\approx -P_{inc}$

(See Pierce p 431)

$P_{total} \simeq 0$

2-6: Backscattering $(\theta = \pi)$

$P_n(\cos\pi) = (-1)^n$ so that the form function becomes (eq. 14):

$$(17) \qquad f(\theta, ka) = \left(\frac{2}{ka}\right)\left|\sum_{n=0}^{\infty} (-1)^n \frac{j_n'(ka)}{h_n'(ka)}(2n+1)\right|$$

A typical plot looks like:

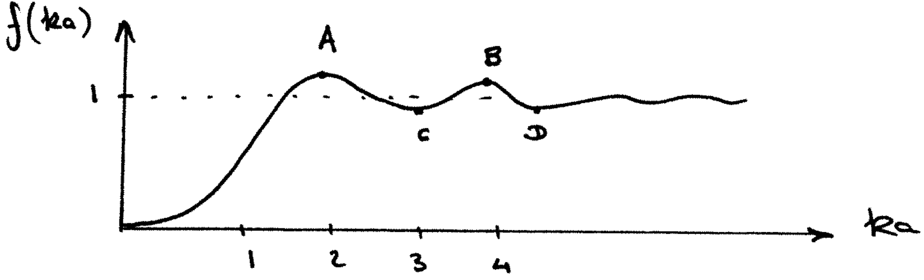

At low (ka), $f(\theta, ka) \rightarrow (ka)^2$

The oscillatory behavior of the function for $ka > 1$ can be interpreted as interference between the specular reflecti (SP) and the waves that "creep" around the sphere (n times) and come back as attenuated "echoes". Thes creeping waves can be in phase (points A and B) o out of phase (points C and D) with the specular reflection.

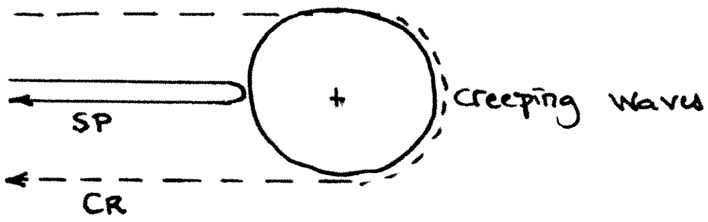

3. Scattering by an elastic sphere

3.1: Boundary conditions

Consider now the case of an elastic sphere.

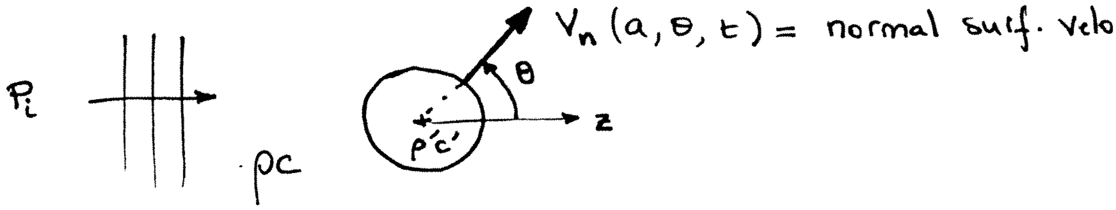

The analysis is exactly the same as for the case of a rigid sphere ($V_n = 0$) except that the boundary condition (4) has to be replaced by Euler's equation evaluated at $r=$ In the case of a time harmonic wave, the pressure-velocity relation at $r=a$ is:

$$(18) \qquad \left[\frac{\partial p}{\partial r}\right]_{r=a} = -j\omega\rho\, V_n(a,\theta,\omega)$$

Such an impedance boundary condition means that, unlike in the case of the rigid sphere, some sound will be transmitted inside the sphere. Let us denote by $P_{tr}(r,\theta,\omega)$ the acoustic pressure inside the sphere The problem can be solved by applying the boundary conditions at the interface $r=a$:

- (i): continuity of pressure
- (ii): continuity of normal particle displacemen

Condition (i) leads to:

$$(19) \qquad P_i(a,\theta) + P_s(a,\theta) = P_{tr}(a,\theta)$$

As for the case of the rigid sphere, we express the incide scattered, and now transmitted fields in terms of the eig functions of the scatterer. This leads to:

(20)

$$P_i(r,\theta,t) = P_0 e^{j(wt-kz)} = P_0 \sum_{n=0}^{\infty} (-j)^n (2n+1) j_n(kr) P_n(\cos\theta$$

$$r \geq a \qquad P_s(r,\theta,t) = \sum_{n=0}^{\infty} b_n h_n^{(2)}(kr) P_n(\cos\theta) e^{jwt}$$

$$r \leq a \qquad P_{tr}(r,\theta,t) = \sum_{n=0}^{\infty} \beta_n j_n(k'r) P_n(\cos\theta) e^{jwt}$$

Note that the Neumann's function $n_n(k'r)$ has been discard to represent the pressure inside the sphere because the pressure must remain finite at $r=0$. Note also that the wavenumbe inside the sphere, k', differs from the wavenumber outside the sphere, k, because c' inside is a priori different fro c outside. Substituting (20) into (19) yields

(21)

$$P_0 \sum_n (-j)^n (2n+1) j_n(ka) P_n(\cos\theta) + \sum_n b_n h_n(ka) P_n(\cos\theta)$$

$$= \sum_n \beta_n j_n(k'a) P_n(\cos\theta)$$

~~which is a generalization of eq. (5) to elastic scattering~~.

The Legendre polynomials being orthogonal, it follows that

(22) $$P_0 (-j)^n (2n+1)\, j_n (ka) + b_n\, h_n (ka) = \beta_n\, j_n (k'a)$$

To determine the coefficients b_n and β_n we need another equation. It is the continuity of normal particle velocity which follows from boundary condition (ii).

$$V_{out}(a,\theta) = V_{in}(a,\theta)$$

or, using (18), $$V_{out}(a,\theta) = -\frac{1}{j\omega\rho}\left(\frac{\partial p_{out}}{\partial r}\right)_{r=a} = -\frac{1}{j\omega\rho'}\left(\frac{\partial p_{in}}{\partial r}\right.$$

Since $p_{out} \equiv p_i + p_s$, and $p_{in} \equiv p_t$, we have

$$\frac{1}{\rho} k P_0 \sum_n (-j)^n (2n+1)\, j_n'(ka)\, P_n(\cos\theta) + \frac{1}{\rho} k \sum_n b_n\, h_n'(ka)\, P_n(\mathrm{co}$$

$$= \frac{1}{\rho'} k' \sum_n \beta_n\, j_n'(ka)\, P_n(\cos\theta)$$

Using the orthogonality of the Legendre polynomials, the above equation has to be satisfied independently at each order n:

(23) $$P_0 (-j)^n (2n+1)\, j_n'(ka) + b_n\, h_n'(ka) = \gamma \beta_n\, j_n'(k'a)$$

where $\gamma = \rho c / \rho' c'$.

Equation (23) is a generalization of eq. (5) to elastic scattering.

Equation (22) and (23) are rewritten with the driving term (the incident sound field) on the RHS:

(24)
$$\left\{\begin{array}{ll} \beta_n j_n(k'a) - b_n h_n(ka) = P_0 (-j)^n (2n+1) j_n(ka) & \text{(pressure} \\ \gamma \beta_n j_n'(k'a) - b_n h_n'(ka) = P_0 (-j)^n (2n+1) j_n'(ka) & \text{(part.} \end{array}\right.$$

3.2. Scattered pressure.

The scattered pressure (and transmitted pressure) can b found explicitely by solving eq. (24) for the coefficients b_n and β_n and plugging them back into eq. (20). Kramer's rule on the system (24) leads to:

(25)
$$\boxed{\begin{gathered} b_n = -(j)^n (2n+1) P_0 \, \mathrm{Det}_n(ka) \\ \text{with} \qquad \mathrm{Det}_n(ka) = \frac{\begin{vmatrix} j_n(k'a) & j_n(ka) \\ \gamma j_n'(k'a) & j_n'(ka) \end{vmatrix}}{\begin{vmatrix} j_n(k'a) & h_n(ka) \\ \gamma j_n'(k'a) & h_n'(ka) \end{vmatrix}} \end{gathered}}$$

A similar expression can be obtained for β_n. Note that for a rigid sphere, $\gamma \rightarrow 0$, and the b_n coefficients reduce to those for the rigid sphere (see eq. (7)).

The farfield approximation for elastic scattering is (see eq.(8

(26) $$\boxed{P_s(r,\theta,t) = -j\,P_o\left[\frac{e^{j(\omega t - kr)}}{kr}\right]\sum_{n=0}^{\infty}(2n+1)\,Det_n(ka)\,P_n(\cos}$$

3.3. Low-ka approximation.

The Rayleigh scattering regime is found by using the asymptotic formulas given in section 2.4. It can easily be shown that, as for the rigid sphere, the first two terms in the series are of order $(ka)^3$ and terms of order $n > 1$ are of order $(ka)^{2n+1}$.

The $n=0$ term (monopole term) is:

$$Det_0(ka) = \frac{j_0(k'a)\,j_0'(ka) - \gamma\,j_0'(k'a)\,j_0(ka)}{j_0(k'a)\,h_0'(ka) - \gamma\,j_0'(k'a)\,h_0(ka)}$$

$$Det_0(ka) = \frac{-\left(\frac{ka}{3}\right)1 - \gamma\left(-\frac{k'a}{3}\right)1}{1\cdot\left(\frac{-j}{(ka)^2}\right) - \gamma\underset{\text{small}}{\cancel{\left(-\frac{k'a}{3}\right)}}\left(\frac{j}{ka}\right)}$$

$$Det_0(ka) = j\,\frac{(ka)^3}{3}\left[-1 + \gamma\,\frac{k'}{k}\right]$$

(27) $$Det_0(ka) = -j\,\frac{(ka)^3}{3}\left[1 - \frac{\rho c^2}{\rho' c'^2}\right]$$

and, similarly, one can show that the $m = 1$ (dipole te
is :

(28). $$\mathrm{Det}_1(ka) = -j\,\frac{(ka)^3}{3}\left[\frac{1-(\rho'/\rho)}{1+2(\rho'/\rho)}\right]$$

Substituting (27) and (28) into (26) yields the final result for the scattered pressure in the farfield and low-ka approximation.

(29) $$\boxed{P_s(r,\theta,t) = P_0\left(\frac{a}{r}\right)(ka)^2 e^{j(\omega t-kr)}\left\{\frac{1-\left(\frac{\rho'c'^2}{\rho c^2}\right)}{3\left(\frac{\rho'c'^2}{\rho c^2}\right)} - \frac{1-\left(\frac{\rho'}{\rho}\right)}{1+2\left(\frac{\rho'}{\rho}\right)}\cos\theta\right.}$$

Again, it appears that in the Rayleigh regime,

- $P_s \propto (ka)^2$
- P_s = (monopole + dipole) terms.

Note that the monopole term is governed by the ratio of the compressibility of the outside and inside media:

$B = \rho c^2$ ⟶

(SPRING EFFECT)

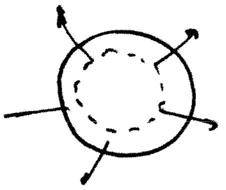

related to ΔV → mo

The dipole term is governed by the ratio of the densities of the outside and inside media; i.e mass controlled, inertia controlled.

(Mass effect).

Again, here, one ignores the higher order terms $n=2,3,\ldots$ in eq. 26 because they are higher order in ka.

The form function becomes:

(30) $$f(\theta, ka) = \left(\frac{2}{ka}\right) \left| \sum_{n=0}^{\infty} (2n+1) \, Det_n \, (ka) \, P_n \, (\cos\theta) \right|$$

with Det_n (ka) defined by eq. (25). Equation (30) is a generalization of eq. (14) to elastic scattering.

3. 4. Scattering by an air bubble in water

We re-examine in more detail eq. (25) at low ka.

Since $$\begin{cases} h_0 \, (ka) = j_0 \, (ka) - j \, n_0 \, (ka) \\ h_0' \, (ka) = j_0' \, (ka) - j \, n_0' \, (ka) \end{cases}$$

$$Det_0 \, (ka) = \frac{j_0 (k'a) \, j_0' \, (ka) - \gamma \, j_0 \, (ka) \, j_0' \, (k'a)}{\left[j_0 (k'a) \, j_0' \, (ka) - \gamma \, j_0 \, (ka) \, j_0' (k'a) \right] - j \left[j_0 (k'a) \, n_0' \, (ka) - \gamma \, j_0' (k'a) \, n \right.}$$

In the low ka limit, it becomes:

$$Det_0 \, (ka) = \frac{-\left(\frac{ka}{3}\right) + \gamma \left(\frac{k'a}{3}\right)}{-\left(\frac{ka}{3}\right) + \gamma \left(\frac{k'a}{3}\right) - j \left[\frac{1}{(ka)^2} - \gamma \left(-\frac{k'a}{3}\right) \left(\frac{-1}{ka}\right) \right]}$$

For an air bubble in water $\gamma = \frac{1.5 \; 10^6}{1.2 \;\; 340} \simeq 3.5 \; 10^3 \gg 1$

31) So $$Det_0 \, (ka) \simeq \frac{\gamma \left(\frac{k'a}{3}\right)}{\gamma \left(\frac{k'a}{3}\right) - j \left[\frac{1}{(ka)^2} - \gamma \, \frac{k'}{3k} \right]}$$

Note again that $\gamma \frac{k'}{k} = \frac{\rho c^2}{\rho' c'^2}$ = ratio of bulk moduli

Note that eq. (31) has the same form as the expression describing the response of a forced, damped, harmonic oscillator. The real part of the denominator corresponds to a damping term:

$$\longrightarrow \quad \frac{1}{3} \frac{\rho c}{\rho' c'} (k' a) = \underline{\text{damping due to radiation of so}}$$

The imaginary part represents the (inertia / compressibility) term i.e. the mass / spring term. Very large pressures can be expected when this term goes to zero. This resonance effect occurs at a frequency such that:

$$\frac{1}{(ka)^2} = \frac{\rho c^2}{3 \rho' c'^2} \quad \rightarrow \quad \left(\frac{2\pi f_{res}}{\cancel{c}} a \right)^2 = \frac{\rho' c'^2}{\rho \cancel{c^2}}$$

(32) or $$\boxed{f_{res} = \frac{c'}{2\pi a} \sqrt{\frac{3\rho'}{\rho}}}$$

① if bubble is small, surface tension is also a restoring force (on top of th compressibility of the gas).

② if bubble is small, adiabatic assumption is not longer valid.

A better formula is: $$\boxed{f_{res} = \frac{c'}{2\pi a} \sqrt{\frac{3\rho'}{\rho}(1+\epsilon)}}$$

ϵ: thermoviscous effects

See Clay & Medwin's <u>Ocean Acoustics</u>, Appendix A-6.

Why do we consider only the $n=0$ mode (monopole) and not even the dipole mode $(n=1)$ in the scattering from a small bubble?

Even though they are both of same order in (ka), the two terms are quite different in magnitudes:

$$P_s = P_0\left(\frac{a}{r}\right)(ka)^2 e^{j(\omega t-kr)}\left\{\frac{1-\frac{\rho'c'^2}{\rho c^2}}{3\left(\frac{\rho'c'^2}{\rho c^2}\right)} - \frac{1-\frac{\rho'}{\rho}}{1+2\frac{\rho'}{\rho}}\cos\theta\right\}$$

$$\rho'c'^2 = 1.2 \times (344)^2 = 1.42 \times 10^5$$

$$\rho c^2 = 10^3 \times (1.5\times 10^3)^2 = 2.25\times 10^9$$

$$\rightarrow \text{ratio} = 6.3\times 10^{-5}$$

$$\frac{\rho'}{\rho} = \frac{1.2}{10^3} = 1.2\times 10^{-3}$$

$$\{\ \ \} \rightarrow \left\{\frac{1}{3\left(6.3\times 10^{-5}\right)} - 1\cos\theta\right\} \rightarrow \underline{\underline{1.9\times 10^6}} - \cos\theta .$$

Appendix:

In this appendix, we derive an expression for the coefficients a_n in the plane wave expansion in spherical coordinates:

$$(1) \qquad \boxed{e^{j(\omega t - kz)} = e^{j\omega t} \sum_{n=0}^{\infty} a_n\, j_n(kr)\, P_n(\cos\theta)}$$

(z = r c

and we show that $a_n = (-j)^n (2n+1)$.

From (1): $\displaystyle\int_{-1}^{1} e^{-jkr\cos\theta}\, P_m(\cos\theta) = \sum a_n\, j_n(kr) \underbrace{\int_{-1}^{1} P_n(\cos\theta)\, P_m(\cos\theta)}_{\left(\frac{2}{2n+1}\right)\delta_{mn}}$

Therefore: $\displaystyle a_n\, j_n(kr) = \left(\frac{2n+1}{2}\right) \int_{-1}^{1} e^{-jkr\cos\theta}\, P_n(\cos\theta)\, d(\cos\theta)$. (

Now, we differentiate n times with respect to kr; set $r=0$ to eliminate the r dependence (since (2) is true at any r).

$$\frac{d^n}{d(kr)^n}\left(a_n\, j_n(kr)\right)_{r=0} = \frac{2n+1}{2} \int_{-1}^{1} (-j\cos\theta)^n\, P_n(\cos\theta)\, d(\cos\theta)$$

$$= \frac{2n+1}{2}\, (-j)^n\, \frac{2^{n+1}\, (n!)^2}{(2n+1)!} \qquad \text{(from Tables}$$

$$(2) \qquad \text{So} \quad a_n = \left[\frac{d^n}{d(kr)^n}\left(j_n(kr)\right)\right]^{-1}_{r=0} \times \left(\frac{2n+1}{2}\right)(-j)^n\, \frac{2^{n+1}\, (n!)^2}{(2n+1)!}$$

But, by definition, $j_n(kr) = 2(kr)^n \sum_{m=0}^{\infty} \frac{(-1)^m (m+n)! \, (kr)^{2m}}{m! \, (2m+2n+1)!}$

so that $$\frac{d^n}{d(kr)^n}\left[j_n(kr)\right] = 2^n \left\{ n! \sum_{m=0}^{\infty} \frac{(-1)^m (m+n)! \, (kr)^{2m}}{m! \, (2m+2n+1)!} \right.$$
$$+ (kr)^n \frac{d}{d(kr)^n}\left[\sum_{m=0}^{\infty} \frac{(-1)^m (m+n)! \, (kr)^{2m}}{m! \, (2m+2n+1)!}\right]$$

so, in the limit $kr \to 0$, the second term vanishes (except when $n=0$) and

$$\frac{d^n}{d(kr)^n}\left[j_n(kr)\right]_{kr=0} = 2^n \, n! \, \frac{n!}{(2n+1)!} = 2^n \frac{(n!)^2}{(2n+1)!}$$

So, in eq. (2): $$a_n = \left(\frac{2n+1}{2}\right)(-j)^n \, \frac{2^{n+1} \, (n!)^2}{(2n+1)!} \, \frac{(2n+1)!}{2^n \, (n!)^2}$$

or $$a_n = \frac{(2n+1)}{2} \, 2 \, (-j)^n$$

$$\boxed{a_n = (-j)^n (2n+1)}$$

Scattering Cross Section

Warning: Definitions may vary by a factor 4π between authors. Here we use Pierce's notation which is a direct analogy with radar theory.

Scattered intensity (time averaged) = $I_{sc} \propto \frac{1}{r^2}$ in farfiel

Incident intensity (") = $I_i \propto 1/r^0$ plane wa

Define the ratio $$\boxed{\left(\frac{d\sigma}{d\Omega}\right) \equiv \left(\frac{I_{sc}(\theta,\phi)}{I_i}\right) r^2}$$

$\left(\frac{d\sigma}{d\Omega}\right) \equiv$ differential scattering cross section.

↓

(per unit solid angle: $d\Omega$)

Note: $\frac{d\sigma}{d\Omega}$ = function of θ, ϕ (and ka) but not of r

The scattering cross section. $$\boxed{\sigma = \int_{4\pi} \left(\frac{d\sigma}{d\Omega}\right) d\Omega}$$

so $$\sigma = \int_{4\pi} \left(\frac{I_{sc}}{I_i}\right) r^2 \sin\theta \, d\theta \, d\phi = \frac{\text{scattered power}}{\text{inc. intensity}} = 1$$

NB: σ can be understood as an "equivalent" or "apparent area blocking the incident wave.

$$\sigma = \int \frac{\frac{1}{\cancel{2\rho c}} |\hat{P}_{sc}|^2}{\frac{1}{\cancel{2\rho c}} |P_0|^2} r^2 \sin\theta \, d\theta \, d\phi = \int \left[\frac{|P_{sc}|_{\infty} r}{P_0} \right]^2 \underbrace{\sin\theta \, d\theta}_{d\Omega}$$

But $\dfrac{|P_{sc}|_{\infty} r}{P_0} \equiv \dfrac{a}{2} f(\theta, \phi, ka)$ form functi

so

$$\boxed{\sigma = \int_{4\pi} \left[\frac{a}{2} f(\theta, \phi) \right]^2 d\Omega}$$

If omnidirectional scattering $f(\theta, \phi) = f_0$

and $\sigma = \dfrac{a^2}{4} f_0^2 \, 4\pi = \pi a^2 f_0^2 = \boxed{\pi a_s^2 = \sigma}$

with $a_s = a f_0$.

Example : the small bubble in water.

If $ka \ll 1$, Rayleigh Scattering. the bubble scatters a spherically symmetrical pressure ; i.e. we may consider only the $n = 0$ mode :

$$f_0(\theta, ka) = \left(\frac{2}{ka}\right) \left| Det_0(ka) \right| \qquad \text{(eq. 30)}$$

with

$$Det_0(ka) = \frac{\gamma \left(\frac{k'a}{3}\right)}{\gamma \left(\frac{k'a}{3}\right) - j \left[\frac{1}{(ka)^2} - \gamma \frac{k'}{3k} \right]} \qquad \text{(eq. 31)}$$

$$|Det(ka)| = \left| \frac{1}{1 - jy} \right| = \frac{1}{\sqrt{1+y^2}} ; \quad y = \frac{\frac{1}{(ka)^2} - \gamma \left(\frac{k'}{3k}\right)}{\gamma \left(\frac{k'a}{3}\right)}$$

so $$\sigma = \pi a^2 \left[\overbrace{\frac{4}{(ka)^2} \quad \frac{1}{1+y^2}}^{f_0^2} \right] = \frac{4\pi a^2}{(ka)^2 + (kay)^2}$$

$$\boxed{\sigma = \frac{4\pi a^2}{\delta^2 + \left[\left(\frac{f_{res}}{f}\right)^2 - 1 \right]^2}}$$

$y = 0$ when $f = f_{res}$
$\delta = ka$.

δ = damping of oscillation . $(\ll 1)$ $= \frac{1}{Q}$

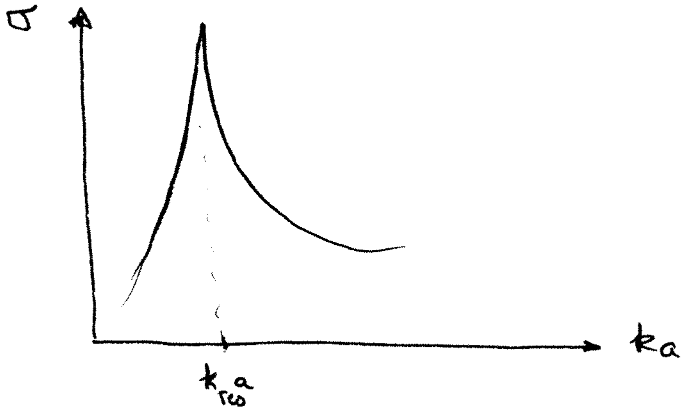

$Q \gg 1$.

Backscattered cross-section : $\sigma_{back} \equiv 4\pi \left(\frac{d\sigma}{d\Omega}\right) = 4\pi \left(\frac{I_{sc}(\theta=\pi)}{I_i} \right) . r^2$

$\rightarrow \theta = \pi$

Bistatic cross-section :

$$\sigma_{bi} = 4\pi \left(\frac{d\sigma}{d\Omega}\right) = 4\pi \left(\frac{I_{sc}}{I_i}\right) . r^2 ,$$

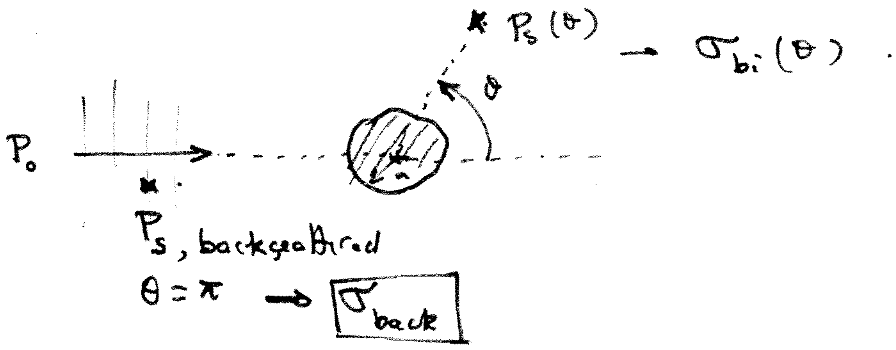

Target Strength :

$$\boxed{TS = 10 \log_{10} \left(\frac{\sigma_{back}}{4\pi R_{ref}^2} \right)}$$

Usually $R_{ref} = 1\,m$.

$$TS = 10 \log_{0} \left[\left(\frac{|\hat{p}_s|^2}{p_0^2} \cdot r^2 \right) 4\pi \times \frac{1}{4\pi R_{ref}^2} \right]$$

$$\boxed{TS = L_p(back, r) - L_p(inc) + 20 \log_{10} \left(\frac{r}{R_{ref}} \right)}$$

$$L_p(back, r) = 20 \log \left(\frac{|\hat{p}_s|}{p_{ref}} \right) \quad @ \; r$$

Resonance & Total Scattering cross section for a "real" bubble.

See Clay & Medwin, Acoustical Oceanography, Wiley 1977. Appendix

$$\boxed{\sigma = 4\pi r^2 \frac{|P_s(r)|^2}{|P_i|^2} = \frac{4\pi a^2}{\left[\left(\frac{f_{res}}{f}\right)^2 - 1\right]^2 + \delta^2}} \quad (1)$$

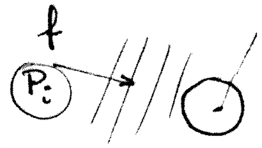

→ δ = damping constant $= \delta_{rad} + \delta_{th} + \delta_{visc}$. (2)

δ_{rad} = due to sound reradiation
δ_{th} = due to thermal conductivity. (small volume ⇒ h
transfer
δ_{visc} = due to viscosity

(3) $\cdot\ \delta_{rad} = ka$

(4) $\cdot\ \delta_{th} = \left(\frac{d}{b}\right)\left(\frac{f_{res}}{f}\right)^2$; d/b = thermal ratio constant (see belo
f_{res} = res. freq. (see below).

(5) $\cdot\ \delta_{visc} = \frac{4\mu}{\rho_A \omega a^2}$;

- μ = dyn. coef. of shear viscosi
(= 0.01 g/cm.s for water
- $\omega = 2\pi f$ (driving frequen
- a = bubble radius
- ρ_A = density of ext. fluid
(= 10^3 kg/m³ for water)

$$\left(\frac{d}{b}\right) = 3(\gamma-1)\left[\frac{X(\sinh X + \sin X) - 2(\cosh X - \cos X)}{X^2(\cosh X - \cos X) + 3(\gamma-1)X(\sinh X - \sin X)}\right]$$

with $$X = a \left[\frac{2\omega \rho_g C_{pg}}{K_g} \right]^{1/2} \qquad (7)$$

with ρ_g = density of bubble gas (see below)
C_{pg} = Specific heat @ constant pressure (of g
($\simeq$ 0.24 cal/g for air)
K_g = Thermal conductivity of gas
($\simeq 5.6\ 10^{-5}$ cal.cm^{-1}.s^{-1}.$(°\text{C})^{-1}$ fo

and $$\rho_g = \rho_{gA} \left[1 + \frac{2\tau}{P_A\, a} \right] (1 + 0.1\, z) \qquad (8)$$

with
- ρ_{gA} = density of free gas @ sea level ($1.29\ 10^{-3}$ g/cm³ for air)
- τ = surface tension ($\simeq$ 75 dynes/cm for air-water)
- P_A = exterior hydrostatic pressure.
- z = depth. (m)

Then compute: $$\boxed{f_{res} = f_{res,0} \times \sqrt{b\beta}} \qquad (9)$$

with $f_{res,0}$ = reson. frequencies w/o thermoviscous effects.

$$\boxed{f_{res,0} = \frac{c'}{2\pi a} \sqrt{\frac{3\rho'}{\rho}} = \frac{1}{2\pi a} \sqrt{\frac{3\gamma P_A}{\rho_A}}} \qquad (10)$$

and $\sqrt{b\beta}$ given by:

- $$b = \left[1+\left(\frac{d}{b}\right)^2\right]^{-1}\left[1+\frac{3\gamma-1}{X}\;\frac{\sinh X - \sin X}{\cosh X - \cos X}\right]^{-1}$$

and

- $$\beta = 1 + \frac{2\tau}{P_A\, a}\left(1-\frac{1}{3\gamma b}\right) \qquad (12).$$

Procedure:

input: ρ_{gA}, τ, P_A, a, z, f, c_{pg}, K_g, γ,

Compute:

ρ_g	eq (8)
X	eq (7)
(d/b)	eq. (6)
b	eq. (11)
β	eq. (12)
f_{res}	eq (10) and (9)
δ_{th}	eq. (4)
δ_{visc}	eq. (5)
δ_{rad}	eq. (3)
δ	eq. (2)
σ	eq. (1).

when $f \to f_{res}$, $\sigma = \frac{4\pi a^2}{\delta^2}$

$\delta = \delta_r + \delta_{th} + \delta_v$

$\delta_r \propto \omega$ high freq.

$\delta_v \propto \frac{1}{\omega}$ low freq

$\delta_{th} \propto$ see eq. (5) mid freq.

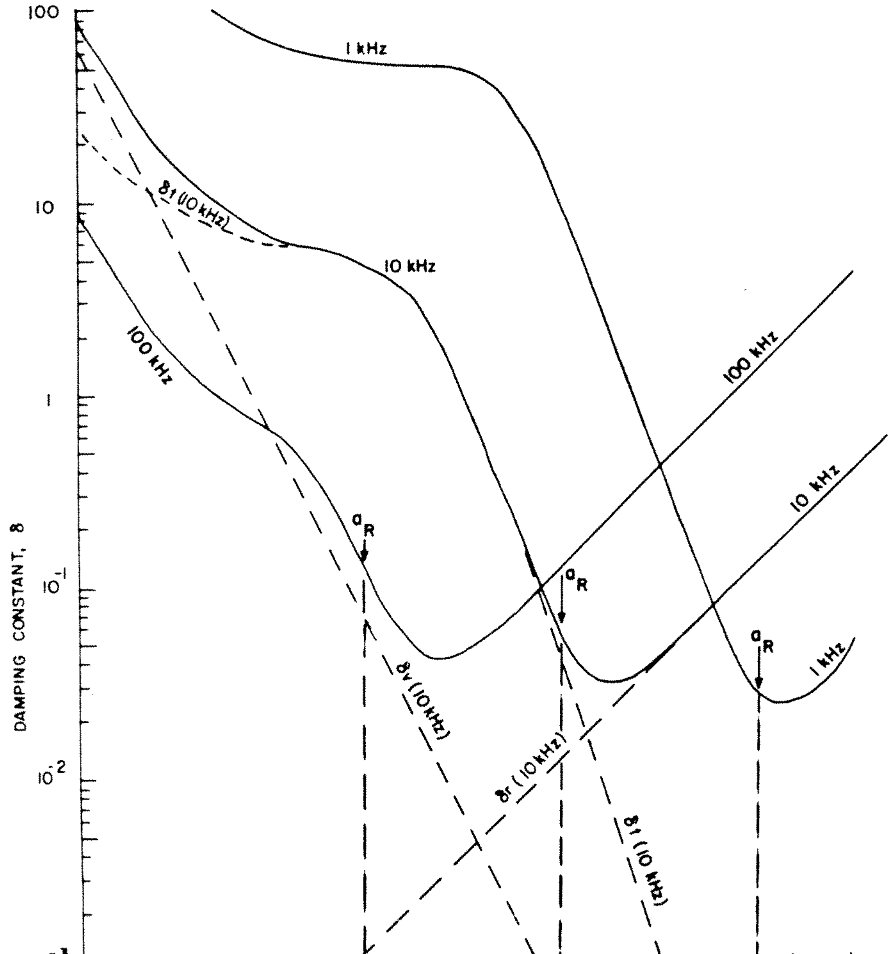

Figure A6.1.2 Damping constants of air bubbles at sea level as a function of bubble radius for three sound frequencies: contributing parts δ_v, δ_t, δ_r are shown for 10 kHz curve; resonance radii a_R are given for three frequencies. The damping constants at resonance δ_R are not the minimum values of δ.

to the compressibility of the pure liquid phase to give a complex summed compressibility. This can be substituted into the expression $\sqrt{B/\rho}$ to give the ratio ω/k_c^{comp}, where k_c^{comp} is the complex wavenumber of the bubbly liquid, the real component of which yields the physical sound speed of the bubbly mixture.

In just such a way, effective analogues of key pure liquid parameters are employed to describe propagation in bubbly mixtures [202, 203], the predictions being in good agreement with experiment [204]. Lu *et al.* [205] present a linearised version of the model, approximating the bubble pulsations to the simple harmonic, which gives results applicable to void fractions of up to a few per cent.

In Chapter 4, section 4.1.2(e) the complex wavenumber k_c^{comp} of sound in a medium containing a uniform distribution of bubbles, all of radius R_o, is found using linearised theory in the limit of small-amplitude oscillations in bubble radius and pressure. Following the discussions of Chapter 1, section 1.1.7, whilst the imaginary part of the wavenumber describes the attenuation, the real part of k_c^{comp} gives the speed of sound in the bubbly medium, $c_c = \omega/\mathrm{Re}\{k_c^{comp}\}$. The result is that in general the speed of sound in a bubbly liquid depends on the size and number of bubbles, and on the frequency of the sound. The presence of bubbles therefore will make the liquid dispersive.[63] The formulation reduces to simple forms when the acoustic frequency and number density of bubbles take extreme values. In the limit of low acoustic frequencies and high number densities, the sound speed in a bubble cloud is (from equation (4.50))

$$c_c \approx \sqrt{\frac{\omega_o^2}{4\pi n_b R_o}} \tag{3.283}$$

which, if ω_M from equation (3.38) is used to approximate for ω_o, reduces to

$$c_c \approx \sqrt{\frac{3\kappa p_o}{\rho n_b(4\pi R_o^3/3)}} \approx \sqrt{\frac{\kappa p_o}{\rho\{\mathrm{VF}\}}} \tag{3.284}$$

giving in the isothermal case

$$c_c \approx \sqrt{\frac{p_o}{\rho\{\mathrm{VF}\}}} \tag{3.285}$$

where {VF} is the 'void fraction' (strictly the gas-volume fraction) [206–208].

In the opposite limit of low number densities, the sound speed is given by equation (4.53):

$$c_c \approx c\left\{1 - (2\pi c^2 n_b R_o)\left(\frac{\omega_o^2 - \omega^2}{(\omega_o^2 - \omega^2)^2 + 4\beta^2\omega^2}\right)\right\} \tag{3.286}$$

where β represents the dissipation.[64] Substitution can be made for a dimensionless damping constant for a single bubble $d = 2\beta/\omega$, which is the off-resonance equivalent of $\delta = 2\beta/\omega_o$. This gives the sound speed in a cloud of bubbles, all of radius R_o, number density n_b, to be

---

[63] See Chapter 1, sections 1.1.1(a) and 1.2.3(c).

$$c_c = c\left\{1 - \left(\frac{2\pi R_o n_b c^2}{\omega^2}\right)\left(\frac{(\omega_o/\omega)^2 - 1}{\{(\omega_o/\omega)^2 - 1\}^2 + d^2}\right)\right\} \tag{3.287}$$

in the limit of low number density. If there is a distribution of bubble sizes within the cloud, such that $n_b^{gr}(z,R_o)\mathrm{d}R_o$ is the number of bubbles per unit volume at depth z having radii between R_o and $R_o + \mathrm{d}R_o$, the speed of sound is a function of both the depth and the acoustic frequency [27]:

$$c_c(z,\omega) = c\left\{1 - (2\pi c^2)\int_{R_o=0}^{\infty} \frac{R_o}{\omega^2}\left(\frac{(\omega_o/\omega)^2 - 1}{\{(\omega_o/\omega)^2 - 1\}^2 + d^2}\right) n_b^{gr}(z,R_o)\mathrm{d}R_o\right\} \tag{3.288}$$

For low insonation frequencies ($\omega \ll \omega_o$), equation (3.287) reduces to

$$c_c = c\left\{1 - \left(\frac{2\pi R_o n_b c^2}{\omega_o^2}\right)\right\} \approx c\left\{1 - \tfrac{1}{2}\{\mathrm{VF}\}\,\frac{\rho c^2}{\kappa p_o}\right\} \tag{3.289}$$

using the approximation $\omega_M \approx \omega_o$.

(ii) The Effect of Vertical Variations in Bubble Population on Sound Speed. The above discussion illustrates how the speed of sound in the ocean can depend on the bubble population, in general the presence of bubbles decreasing the sound speed. Because of this effect, an alternative explanation to that of Longuet-Higgins for the presence of peaks in the acoustic spectrum in the sea has been proposed by Farmer and Vagle [66]. They suggest that waveguide propagation may occur in the ocean-surface bubble layer. Bubbles are entrained from the free surface of the ocean, so as the concentration of bubbles decreases with depth in the bubble-rich first few metres below the surface, the sound speed increases. If, for whatever reason, the sound speed increases with depth, sound waves propagating downwards will tend to turn, propagating at angles closer to the horizontal. This can be seen by using a construction of Huygen's wavelets for the sound, much as was done in Figure 1.3 for water waves approaching a beach, to show how a wavefront will turn as it progresses. Figure 3.61 shows how, if the sound speed increases with depth, sound initially propagating down from the surface may be refracted upwards towards the surface, from which it will reflect downwards. Repetition of this cycle can trap acoustic energy in a near-surface region [209, 210]. A wave of frequency greater than around 2 kHz might propagate through such a waveguide or duct, though scattering and absorption by bubbles, and the presence of bubble clouds and an irregular sea surface, might cause attenuation [146]. Farmer and Vagle [66] postulated, as a result of their analysing the frequency components of ambient ocean noise, that the trapping of sound in such a waveguide might influence the ambient acoustic spectra.

The breaking of a wave will emit sound [26]. Farmer and Vagle [66] video-recorded wave-breaking events at sea, and recorded the resulting sound. The spectrum of this acoustic emission does not exhibit a continuous frequency content, but instead is found to contain fine structure which is coherent over the duration of the event. In addition, the spectral fine structure is similar between one wave-breaking event and the next. The fine structure does vary during a given storm, and between storms. Farmer and Vagle report having observed such structure in a range of spectra measured in different geographic environments, including Georgia Strait

Homework

- Compare with Faran's Fig 6. (not 8 !)
- Faran's notation: mc/s = MHZ

$x_3 = k_3 a$ (in water)

$x_1 = k_1 a$ (inside scatterer).

$k_1 = \frac{\omega}{c_1}$; c_1 = bulk wave speed
able to sustain both
shear & compression waves.

$$c_1 = \sqrt{\frac{\lambda + 2\mu}{\rho}} = \sqrt{\frac{K + \frac{4}{3}\mu}{\rho}}$$

for Brass $c_1 = 4700$ m/s

$x_3 = 3.4$ $x_1 = 1.1$ ✓

- Major difference between your program & Faran:

Faran includes shear waves inside scatterer.
Model solid.
Yours is essentially a fluid ($\rho' c'^2$) scatterer.

GEORGIA INSTITUTE OF TECHNOLOGY
WOODRUFF SCHOOL OF MECHANICAL ENGINEERING

ME 6761 - ACOUSTICS II

Project: - due Friday November 30 in class.

PART I: ANALYTICAL

Consider scattering of sound by an infinite elastic cylinder submerged under water. Starting from the Fourier decomposition of the incident plane wave ($z = r\cos\phi$)

$$P_0 e^{j(\omega t-kz)} = P_0 e^{j\omega t}\sum_{n=0}^{\infty}\varepsilon_n(-j)^n J_n(kr)\cos(n\phi) \qquad (1)$$

where $\varepsilon = 1$ if $n=0$, and $\varepsilon = 2$ if $n \geq 1$, express the scattered and transmitted pressures as

$$p_s(r,\phi,t) = \sum_{n=0}^{\infty} b_n H_n^{(2)}(kr)\cos(n\phi)e^{j\omega t}$$

$$p_t(r,\phi,t) = \sum_{n=0}^{\infty} \beta_n J_n(kr)\cos(n\phi)e^{j\omega t} \quad . \qquad (2)$$

1) Write the boundary conditions at r = a.
2) Find the coefficients b_n and β_n.
3) Derive an expression for the scattered pressure in the farfield in the low *ka* approximation. (Use Abramowitz and Stegun ' reference book for asymptic expressions as necessary).

II. Numerical

far field $kr = 10$

1) Write a numerical program to evaluate the sound field scattered by a 0.0625 inch diameter brass cylinder in water at a frequency of 1 MHz. Compare with Figure ~~8~~ 6 of Faran's paper (J. Acoust. Soc. Am., vol 23, N0 4, p 405-418 (1951).) Discussion.

2) Plot the backscattering for function ($\phi=\pi$) over a frequency range such that $0.1 \le ka \le 6$ for

   $(a)\ \rho'/\rho = c'/c = 0.5$

   $(b)\ \rho'/\rho = c'/c = 10.$ (hard cylinder)

   $(c)\ \rho' = 1.21\ kg/m^3$ and $c' = 344\ m/s.$ (air cylinder)

3) Evaluate the (backscattered) target strength TS at ka=2. Recall,

$$TS = 10\log_{10}\left[\frac{\sigma_b}{A_{ref}}\right];$$

$$\sigma_b = A\ \frac{I_{sc}}{I_i} = (2\pi r L)\left(\frac{I_{sc}}{I_i}\right) = \frac{2\pi \cancel{r} L}{\cancel{r}}\left(\frac{af}{2}\right)^2$$

$$A = 2\pi \overset{r}{\cancel{R}} L = 2\pi r L$$

$$\boxed{L=1}$$

$$\frac{I_{sc}}{I_i} = \left(\frac{P_{sc}}{P_i}\right)^2 = \cancel{\frac{(af/2)^2}{r}}$$

TS per unit length.

$$A_{ref} = 1\ m^2$$

where f is the form function, a the radius of the cylinder, r the distance between the field point (farfield) and the center of the cylinder of length L (assumed very long).

THE JOURNAL
OF THE
ACOUSTICAL SOCIETY OF AMERICA

Volume 23 Number 4

JULY • 1951

Sound Scattering by Solid Cylinders and Spheres*

JAMES J. FARAN, JR.
Acoustics Research Laboratory, Harvard University, Cambridge, Massachusetts

(Received March 13, 1951)

The theory of the scattering of plane waves of sound by isotropic circular cylinders and spheres is extended to take into account the shear waves which can exist (in addition to compressional waves) in scatterers of solid material. The results can be expressed in terms of scattering functions already tabulated. Scattering patterns computed on the basis of the theory are shown to be in good agreement with experimental measurements of the distribution-in-angle of sound scattered in water by metal cylinders. Rapid changes with frequency in the distribution-in-angle of the scattered sound and in the total scattered energy are found to occur near frequencies of normal modes of free vibration of the scattering body.

I. INTRODUCTION

THE scattering of sound was first investigated mathematically by Lord Rayleigh.[1] However, because of the complexity of the mathematical solution, he only considered the limiting case where the scatterers are small compared with the wavelength. The solution for scattering by rigid, immovable circular cylinders and spheres, not necessarily small compared with the wavelength, was given in convenient form by Morse, who defined and tabulated values of phase-angles associated with the partial scattered waves, in order to simplify the complicated dependence on bessel functions.[2] Although most solid scatterers in air can be considered rigid and immovable, it is valid only in a few special cases to assume that a scatterer in a liquid medium is rigid and immovable. In general, the sound waves which penetrate the scatterer must be taken into account, as they can have a considerable effect on the distribution-in-angle of the scattered sound and on the total scattered energy. Morse, with Lowan, Feshbach, and Lax, later extended his solution to include the effects of compressional waves inside (fluid) cylindrical and spherical scatterers.[3] These results are also given in convenient form in terms of several additional phase-angles whose values are tabulated. The object of the research reported here has been to study sound scattering by cylinders and spheres of solid material (which will support shear waves in addition to compressional waves). The mathematical solution will be given first, after which experimental apparatus and results will be described.

II. THE MATHEMATICAL SOLUTION

List of Symbols

Most of the symbols used here are, in the appropriate sections of the analysis, the same as those used by Love and those used by Morse:

a = radius of cylinder or sphere;
a_n, b_n, c_n = expansion coefficients;

---

* This paper contains the essential results of a thesis submitted to the Faculty of Harvard University in partial fulfillment of the requirements for the degree of Doctor of Philosophy. This research has been aided by funds made available under a contract with the ONR.

[1] Lord Rayleigh, *The Theory of Sound* (Dover Publications, New York, 1945), first American edition.

[2] P. M. Morse, *Vibration and Sound* (McGraw-Hill Book Company, New York, 1936), first edition, and (1948), second edition.

[3] Mathematical Tables Project and M.I.T. Underwater Sound Laboratory, *Scattering and Radiation from Circular Cylinders and Spheres* (U. S. Navy Department, Office of Research and Inventions, Washington, D. C., 1946).

$\mathbf{A}$ = vector displacement potential;
A_z = z-component of vector potential;
A_ϕ = ϕ-component of vector potential;
c_1 = velocity of compressional waves in the scatterer;
c_2 = velocity of shear waves in the scatterer;
c_3 = velocity of sound in the fluid surrounding the scatterer;
E = Young's modulus;
j = $(-1)^{\frac{1}{2}}$;
$j_n(\ )$ = spherical bessel function of the first kind;
$J_n(\ )$ = bessel function of the first kind;
k_1 = ω/c_1;
k_2 = ω/c_2;
k_3 = ω/c_3;
n = order integer;
$n_n(\ )$ = spherical bessel function of the second kind;
$N_n(\ )$ = bessel function of the second kind;
p = pressure;
p_i = pressure in incident wave;
p_s = pressure in scattered wave;
$P_n(\cos\theta)$ = Legendre polynomial;
P_0 = amplitude of pressure in incident wave;
r, θ, z = cylindrical coordinates;
r, θ, ϕ = spherical coordinates;
$[rr], [r\theta], [rz]$ = stress components in cylindrical coordinates;
$[rr], [r\theta], [r\phi]$ = stress components in spherical coordinates;
t = time;
$\mathbf{u}$ = displacement;
u_r, u_θ = components of displacement in the solid;
$u_{i,r}$ = radial component of displacement in incident wave;
$u_{s,r}$ = radial component of displacement in scattered wave;
x, y, z = rectangular coordinates;
x_1 = k_1a;
x_2 = k_2a;
x_3 = k_3a;
$\alpha_n, \beta_n, \delta_n, \delta_n', \zeta_n, \eta_n$ = scattering phase-angles;
Δ = dilatation;
ϵ_n = Neumann factor; $\epsilon_0=1$; $\epsilon_n=2$, $n>0$;
λ, μ = Lamé elastic constants;
$2\bar{\omega}$ = rotation;
ρ_1 = density of the scatterer;
ρ_3 = density of the fluid surrounding the scatterer;
σ = Poisson's ratio;
Φ_n = boundary impedance scattering phase-angle;
Ψ = scalar displacement potential;
ω = angular frequency $(2\pi f)$.

Scattering by Solid Circular Cylinders

Plane waves of sound of frequency $\omega/2\pi$ in a fluid medium are incident upon an infinitely long circular cylinder of some isotropic solid material. Let the axis of the cylinder coincide with the z-axis of a rectangular coordinate system, and let the plane wave approach the cylinder along the negative x-axis, as shown in Fig. 1. As in the solutions given previously for rigid and fluid scatterers,[1-3] the wave motion external to the scatterer is assumed to consist of the incident plane wave and an outgoing scattered wave. It is desired to find the amplitude of the scattered wave as measured at large distances from the cylinder. The mathematical expressions for displacement and dilatation inside and for pressure and displacement outside the cylinder will be found in general form first, after which the application of the proper boundary conditions at the surface of the cylinder will lead directly to the solution.

The waves inside the cylinder will be represented by suitable solutions of the equation of motion of a solid elastic medium, which may be written[4]

$$(\lambda+2\mu)\nabla\Delta-\mu\nabla\times(2\bar{\omega})=\rho_1\partial^2\mathbf{u}/\partial t^2, \qquad (1)$$

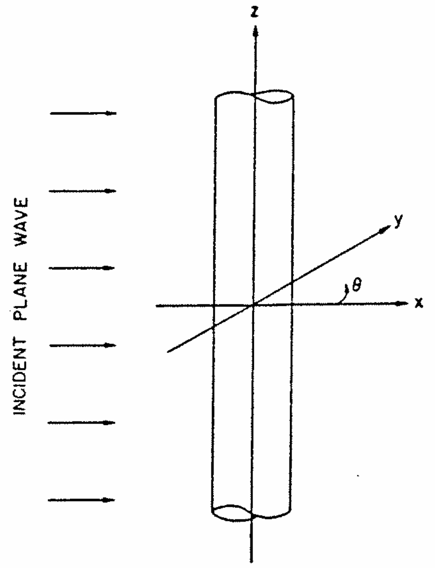

FIG. 1. Choice of coordinate axes for scattering by cylinders.

where

$$\Delta=\nabla\cdot\mathbf{u} \qquad (2)$$

and

$$2\bar{\omega}=\nabla\times\mathbf{u}.$$

From Eq. (1) can be derived the equations,

$$\nabla^2\Delta=(\rho_1/\lambda+2\mu)\partial^2\Delta/\partial t^2 \qquad (3)$$

and

$$\nabla^2(2\bar{\omega})=(\rho_1/\mu)\partial^2(2\bar{\omega})/\partial t^2, \qquad (4)$$

which define the wave velocities

$$c_1=[(\lambda+2\mu)/\rho_1]^{\frac{1}{2}}=[E(1-\sigma)/\rho_1(1+\sigma)(1-2\sigma)]^{\frac{1}{2}} \qquad (5)$$

and

$$c_2=(\mu/\rho_1)^{\frac{1}{2}}=[E/2\rho_1(1+\sigma)]^{\frac{1}{2}}. \qquad (6)$$

Solutions of Eq. (1) can be found by assuming that the

---

[4] A. E. H. Love, *A Treatise on the Mathematical Theory of Elasticity* (Dover Publications, New York, 1944), fourth edition, p. 141.

displacement can be derived from a scalar and a vector potential:

$$\mathbf{u} = -\nabla\Psi + \nabla\times\mathbf{A}. \tag{7}$$

The displacement thus can be thought of as the sum of two displacements, one associated with compressional waves and the other with shear waves. If we assume that the potentials satisfy the equations,

$$\nabla^2\Psi = (1/c_1^2)\partial^2\Psi/\partial t^2 \tag{8}$$

and

$$\nabla^2\mathbf{A} = (1/c_2^2)\partial^2\mathbf{A}/\partial t^2, \tag{9}$$

we can show that $\Delta(=\nabla\cdot(-\nabla\Psi))$ satisfies Eq. (3), and that $2\bar{\omega}(=\nabla\times\nabla\times\mathbf{A})$ satisfies Eq. (4). That these assumptions do lead to a valid solution of Eq. (1) may be seen by noting that the solutions we shall obtain satisfy Eq. (1) by direct substitution. If we now change to a cylindrical coordinate system defined by

$$x = r\cos\theta, \quad y = r\sin\theta, \quad z = z,$$

it can be seen that pressure and displacement must be symmetrical about $\theta=0$ (the direction of the positive x-axis). Moreover, because the cylinder is of infinite length, and the incident plane wave of infinite extent, there can be no dependence on z, and it is logical to assume that there is no displacement in the z-direction. Subject to these conditions, the solution of Eq. (8) can be written

$$\Psi = \sum_{n=0}^{\infty} a_n J_n(k_1 r)\cos n\theta. \tag{10}$$

(The time dependence factor $\exp(j\omega t)$ will be understood in all the expressions representing waves.) Examination of Eq. (9) shows that, subject to the conditions discussed above, the vector potential can have no component in the r- or the θ-direction. The vector Eq. (9) then reduces to a scalar equation in A_z, and its solution can be written

$$A_z = \sum_{n=0}^{\infty} b_n J_n(k_2 r)\sin n\theta. \tag{11}$$

Only sine terms appear here, because the vector potential must be anti-symmetrical about $\theta=0$ in order that the displacement derived from it shall be symmetrical about $\theta=0$. Now, by Eqs. (7) and (2),

$$u_r = \sum_{n=0}^{\infty}\left[\frac{nb_n}{r}J_n(k_2 r) - a_n\frac{d}{dr}J_n(k_1 r)\right]\cos n\theta, \tag{12}$$

$$u_\theta = \sum_{n=0}^{\infty}\left[\frac{na_n}{r}J_n(k_1 r) - b_n\frac{d}{dr}J_n(k_2 r)\right]\sin n\theta, \tag{13}$$

and

$$\Delta = k_1^2\sum_{n=0}^{\infty} a_n J_n(k_1 r)\cos n\theta. \tag{14}$$

The waves in the fluid surrounding the cylinder will be represented by suitable solutions of the wave equation for a (nonviscous) fluid medium, which can be written

$$\nabla^2 p = (1/c_3^2)\partial^2 p/\partial t^2.$$

The incident plane wave is represented by[5]

$$p_i = P_0\exp(-jk_3 x) = P_0\exp(-jk_3 r\cos\theta)$$
$$= P_0\sum_{n=0}^{\infty}\epsilon_n(-j)^n J_n(k_3 r)\cos n\theta. \tag{15}$$

The radial component of displacement associated with this wave is

$$u_{i,r} = (1/\rho_3\omega^2)\partial p_i/\partial r$$
$$= \frac{P_0}{\rho_3\omega^2}\sum_{n=0}^{\infty}\epsilon_n(-j)^n\frac{d}{dr}J_n(k_3 r)\cos n\theta. \tag{16}$$

The outgoing scattered wave must be symmetrical about $\theta=0$ and therefore of the form

$$p_s = \sum_{n=0}^{\infty} c_n[J_n(k_3 r) - jN_n(k_3 r)]\cos n\theta. \tag{17}$$

The radial component of displacement associated with this wave is

$$u_{s,r} = \frac{1}{\rho_3\omega^2}\sum_{n=0}^{\infty} c_n\frac{d}{dr}[J_n(k_3 r) - jN_n(k_3 r)]\cos n\theta. \tag{18}$$

The factors c_n are the unknown coefficients which must be evaluated.

The following boundary conditions are applied at the surface of the cylinder: (I) The pressure in the fluid must be equal to the normal component of stress in the solid at the interface; (II) the normal (radial) component of displacement of the fluid must be equal to the normal component of displacement of the solid at the interface; and (III) the tangential components of shearing stress must vanish at the surface of the solid. That is,

$$p_i + p_s = -[rr] \quad \text{at} \quad r = a, \tag{19}$$

$$u_{i,r} + u_{s,r} = u_r \quad \text{at} \quad r = a, \tag{20}$$

and

$$[r\theta] = [rz] = 0 \quad \text{at} \quad r = a. \tag{21}$$

In cylindrical coordinates,[6]

$$[rr] = \lambda\Delta + 2\mu\partial u_r/\partial r = 2\rho_1 c_2^2[(\sigma/1-2\sigma)\Delta + \partial u_r/\partial r],$$
$$[r\theta] = \mu[(1/r)(\partial u_r/\partial\theta) + (r\partial/\partial r)(u_\theta/r)],$$

and

$$[rz] = \mu[\partial u_r/\partial z + \partial u_z/\partial r].$$

By the conditions of symmetry, $[rz]=0$ everywhere. Upon substitution from Eqs. (15), (17), (14), (12), (16), (18), and (13), the boundary condition Eqs. (19), (20),

---

[5] See reference 2, second edition, p. 347.

[6] See reference 4, p. 288.

and (21) become, for the nth mode,

$$x_1 J_n'(x_1) a_n - n J_n(x_2) b_n + (x_3/\omega^2\rho_3)[J_n'(x_3) - jN_n'(x_3)]c_n = -(P_0 x_3/\omega^2\rho_3)\epsilon_n(-j)^n J_n'(x_3), \quad (19a)$$

$$2\rho_1 c_2^2 x_1^2[(\sigma/1-2\sigma)J_n(x_1) - J_n''(x_1)]a_n + 2\rho_1 c_2^2 n[x_2 J_n'(x_2) - J_n(x_2)]b_n + a^2[J_n(x_3) - jN_n(x_3)]c_n = -P_0\epsilon_n(-j)^n a^2 J_n(x_3), \quad (20a)$$

and

$$2n[x_1 J_n'(x_1) - J_n(x_1)]a_n = [n^2 J_n(x_2) - x_2 J_n'(x_2) + x_2^2 J_n''(x_2)]b_n. \quad (21a)$$

Solving these equations simultaneously for c_n is laborious but straightforward. The result is

$$c_n = -P_0\epsilon_n(-j)^{n+1}\sin\eta_n \exp(j\eta_n), \quad (22)$$

where η_n, the phase-shift angle of the nth scattered wave, is defined by

$$\tan\eta_n = \tan\delta_n(x_3) \times [\tan\Phi_n + \tan\alpha_n(x_3)]/[\tan\Phi_n + \tan\beta_n(x_3)].$$

The intermediate scattering phase-angles

$$\delta_n(x) = \tan^{-1}[-J_n(x)/N_n(x)],$$
$$\alpha_n(x) = \tan^{-1}[-xJ_n'(x)/J_n(x)],$$

and

$$\beta_n(x) = \tan^{-1}[-xN_n'(x)/N_n(x)],$$

have been defined and their values tabulated previously.[3] The angle Φ_n, which is a measure of the boundary impedance at the surface of the scatterer, is given, for a solid scatterer, by

$$\tan\Phi_n = (-\rho_3/\rho_1)\tan\zeta_n(x_1, \sigma), \quad (23)$$

where the new scattering phase-angle $\zeta_n(x_1, \sigma)$ is given by

$$\zeta_n(x_1, \sigma) = \tan^{-1}\left[-\frac{x_2^2}{2}\,\frac{\dfrac{x_1 J_n'(x_1)}{x_1 J_n'(x_1) - J_n(x_1)} - \dfrac{2n^2 J_n(x_2)}{n^2 J_n(x_2) - x_2 J_n'(x_2) + x_2^2 J_n''(x_2)}}{\dfrac{(\sigma/1-2\sigma)x_1^2[J_n(x_1) - J_n''(x_1)]}{x_1 J_n'(x_1) - J_n(x_1)} + \dfrac{2n^2[x_2 J_n'(x_2) - J_n(x_2)]}{n^2 J_n(x_2) - x_2 J_n'(x_2) + x_2^2 J_n''(x_2)}}\right]. \quad (24)$$

For convenience in computing values of this function, it can be written in terms of the angle $\alpha_n(x)$:

$$\zeta_n(x_1, \sigma) = \tan^{-1}\left[-\frac{x_2^2}{2}\,\frac{\dfrac{\tan\alpha_n(x_1)}{\tan\alpha_n(x_1)+1} - \dfrac{n^2}{\tan\alpha_n(x_2) + n^2 - \frac{1}{2}x_2^2}}{\dfrac{\tan\alpha_n(x_1) + n^2 - \frac{1}{2}x_2^2}{\tan\alpha_n(x_1)+1} - \dfrac{n^2[\tan\alpha_n(x_2)+1]}{\tan\alpha_n(x_2) + n^2 - \frac{1}{2}x_2^2}}\right]. \quad (25)$$

Although ζ_n as written above is explicitly a function of x_1 and x_2, it can be considered a function of x_1 and σ, since the ratio of x_1 and x_2 is a function of σ only. Values of $\zeta_n(x_1, \sigma)$ computed from Eq. (25) for $\sigma = \frac{1}{3}$ are given in Table I. For convenience in finding the tangent, the value of the angle lying between ±90° is given in the table. The dotted lines indicate that $\zeta_n(x_1, \sigma)$ passes through ±90° between the adjacent entries, and thus serve to point out the infinities of $\tan\zeta_n(x_1, \sigma)$. It will be seen below that the infinities of $\tan\zeta_n(x_1, \sigma)$ occur at precisely the frequencies of those normal modes of free vibration of the scatterer which satisfy the conditions of symmetry of the scattering problem. The dotted lines in Table I thus mark the locations of the normal modes of vibration of the scatterer. For other values of Poisson's ratio the functions will be similar, the only difference being shifts in the locations of the normal modes.

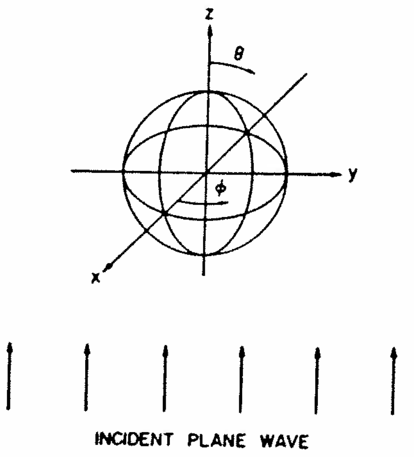

FIG. 2. Choice of coordinate axes for scattering by spheres.

The scattering pattern, or distribution-in-angle of pressure in the scattered wave at large distances from the cylinder, can be found from Eqs. (17) and (22), using the asymptotic expressions for the bessel functions for large arguments:

$$|p_s| \xrightarrow[r\to\infty]{} P_0\left(\frac{2}{\pi k_3 r}\right)^{\frac{1}{2}} \left|\sum_{n=0}^{\infty} \epsilon_n \sin\eta_n \exp(j\eta_n)\cos n\theta\right|. \quad (26)$$

Scattering by Solid Spheres

Let us assume that plane waves of sound in a fluid medium are incident upon a sphere of some isotropic

TABLE I. Values of $\zeta_n(x_1, \sigma)$ for the cylindrical case for $\sigma = \frac{1}{4}$.

$n=0$	$n=1$	$n=2$	$n=3$	$n=4$	$n=5$	$n=6$	$n=7$	$n=8$	$n=9$
0.00°	−45.00°	0.00°	0.00°	0.00°	0.00°	0.00°	0.00°	0.00°	0.00°
1.37	−44.13	3.59	2.06	1.52	1.20	1.01	0.86	0.76	0.67
6.27	−43.33	15.47	8.73	6.33	4.97	4.02	3.46	3.03	2.68
14.35	−41.18	36.24	20.10	14.07	11.15	9.12	7.80	6.80	6.04
25.60	−37.48	60.28	35.26	25.40	19.90	16.24	14.00	12.12	10.24
38.90	−31.24	79.03	51.42	37.95	30.52	25.18	21.23	18.52	16.84
52.22	−18.06	−88.71	65.40	50.79	41.33	34.96	30.31	26.58	23.56
63.81	+62.49	−79.71	76.03	61.87	52.07	45.11	38.96	34.61	31.22
73.08	−31.82	−74.29	83.85	70.71	61.11	53.83	47.93	42.73	39.11
80.33	−7.53	−68.94	89.73	77.52	68.61	61.51	55.74	50.71	46.45
[illegible]6.05	+15.39	−63.54	−85.59	82.84	74.55	67.96	62.24	57.38	53.06
−89.25	36.63	−56.21	−81.57	87.06	79.25	73.05	67.88	63.03	59.43
−85.16	53.17	−49.71	−77.67	−89.43	83.05	77.21	72.25	67.97	64.10
−81.30	64.93	−37.81	−73.08	−86.35	86.22	80.71	76.15	72.17	68.51
−77.32	73.30	−19.43	−64.48	−83.42	88.92	83.58	79.25	75.52	72.15
−72.71	79.69	+6.92	+68.10	−80.28	−88.67	86.02	81.83	78.34	75.20
−66.65	85.83	34.29	−74.64	−76.17	−86.39	88.15	84.09	80.71	77.75
−57.35	74.49	54.21	−65.75	−68.06	−84.05	−89.92	86.04	82.78	79.94
−40.29	87.38	67.25	−55.95	−11.94	−81.35	−88.10	87.77	84.58	81.86
−6.92	−89.02	76.96	−40.24	+85.24	−77.55	−86.28	89.35	86.18	83.57
+34.15	−86.10	−87.62	−11.45	−83.85	−69.80	−84.30	−89.16	87.59	85.03
58.25	−83.24	+70.33	+28.36	−78.33	−27.54	−81.87	−87.69	88.91	86.34
70.32	−80.06	80.59	57.79	−73.27	+75.02	−78.22	−86.15	−89.85	87.54
77.19	−76.03	84.69	78.81	−66.94	88.55	−70.46	−84.38	−88.63	88.64
81.68	−70.05	87.52	14.69	−56.75	−86.36	−29.41	−82.10	−87.38	89.69
84.94	−60.60	89.87	68.66	−34.99	−82.97	+70.97	−78.49	−86.02	−89.28

d m[illegible]rial. Let the center of the sphere coincide with origin of a rectangular coordinate system, and let the ne waves approach the sphere along the negative tis, as shown in Fig. 2. The analysis is very similar to t for the cylindrical case. We transfer to spherical rdinates defined by

$$x = r\sin\theta\cos\phi,\quad y = r\sin\theta\sin\phi,\quad z = r\cos\theta.$$

:ause the incident wave approaches along the axis of there is no dependence on ϕ. It is logical to assume t there is no component of displacement in the irection, and it follows that the only non-zero comıent of the vector potential in this case is A_ϕ. The entials are then found to be of the forms,

$$\Psi = \sum_{n=0}^{\infty} a_n j_n(k_1 r) P_n(\cos\theta)$$

$$A_\phi = \sum_{n=0}^{\infty} b_n j_n(k_2 r) \frac{d}{d\theta} P_n(\cos\theta).$$

Pressure in the incident wave is represented by[7]

$$p_i = P_0 \exp(-jk_3 z) = P_0 \exp(-jk_3 r\cos\theta)$$

$$= P_0 \sum_{n=0}^{\infty} (2n+1)(-j)^n j_n(k_3 r) P_n(\cos\theta).$$

The outgoing scattered wave will be of the form,

$$p_s = \sum_{n=0}^{\infty} c_n[j_n(k_3 r) - jn_n(k_3 r)]P_n(\cos\theta). \qquad (27)$$

The same boundary conditions at the surface of the scatterer are applied to the expressions for displacement, pressure, and dilatation, which are either given above or derivable from the above. In spherical coordinates the stress components are

$$[rr] = \lambda\Delta + 2\mu\partial u_r/\partial r = 2\rho_1 c_2^2[(\sigma/1-2\sigma)\Delta + \partial u_r/\partial r],$$

$$[r\theta] = \mu\left[\frac{\partial u_\theta}{\partial r} - \frac{u_\theta}{r} + \frac{1}{r}\frac{\partial u_r}{\partial\theta}\right],$$

---

[7] See reference 2, second edition, p. 354.

and

$$[r\phi]=\mu\left[\frac{1}{r\sin\theta}\frac{\partial u_r}{\partial\theta}+\frac{\partial u_\phi}{\partial r}-\frac{u_\phi}{r}\right].$$

By carrying the analysis through as in the cylindrical case, we find that

$$c_n=-P_0(2n+1)(-j)^{n+1}\sin\eta_n\exp(j\eta_n), \quad (28)$$

where the phase-shift η_n of the nth scattered wave is defined by

$$\tan\eta_n=\tan\delta_n(x_3)[\tan\Phi_n+\tan\alpha_n(x_3)]/\tan\Phi_n+\tan\beta_n(x_3).$$

The intermediate angles,

$$\delta_n(x)=\tan^{-1}[-j_n(x)/n_n(x)],$$
$$\alpha_n(x)=\tan^{-1}[-xj_n'(x)/j_n(x)],$$
$$\beta_n(x)=\tan^{-1}[-xn_n'(x)/n_n(x)],$$

have been defined and their values tabulated previously.[8] The boundary impedance phase-angle Φ_n is defined by

$$\tan\Phi_n=-(\rho_3/\rho_1)\tan\zeta_n(x_1,\sigma), \quad (29)$$

where the new scattering phase angle $\zeta_n(x_1,\sigma)$ is given by

$$\zeta_n(x_1,\sigma)=\tan^{-1}\left[-\frac{x_2^2}{2}\frac{\dfrac{x_1j_n'(x_1)}{x_1j_n'(x_1)-j_n(x_1)}-\dfrac{2(n^2+n)j_n(x_2)}{(n^2+n-2)j_n(x_2)+x_2^2j_n''(x_2)}}{\dfrac{(\sigma/1-2\sigma)x_1^2[j_n(x_1)-j_n''(x_1)]}{x_1j_n'(x_1)-j_n(x_1)}-\dfrac{2(n^2+n)[j_n(x_2)-x_2j_n'(x_2)]}{(n^2+n-2)j_n(x_2)+x_2^2j_n''(x_2)}}\right].$$

This function can be expressed in terms of the angle $\alpha_n(x)$:

$$\zeta_n(x_1,\sigma)=\tan^{-1}\left[-\frac{x_2^2}{2}\frac{\dfrac{\tan\alpha_n(x_1)}{\tan\alpha_n(x_1)+1}-\dfrac{n^2+n}{n^2+n-1-\frac{1}{2}x_2^2+\tan\alpha_n(x_2)}}{\dfrac{n^2+n-\frac{1}{2}x_2^2+2\tan\alpha_n(x_1)}{\tan\alpha_n(x_1)+1}-\dfrac{(n^2+n)[\tan\alpha_n(x_2)+1]}{n^2+n-1-\frac{1}{2}x_2^2+\tan\alpha_n(x_2)}}\right]. \quad (30)$$

Values of this function computed from Eq. (30) for $\sigma=\frac{1}{3}$ are given in Table II. The dotted lines again indicate the infinities of $\tan\zeta_n(x_1,\sigma)$, that is, the normal modes of free vibration of the scatterer.

The distribution in angle of pressure in the scattered wave at large distances from the sphere is found from Eqs. (27) and (28) by means of the asymptotic expressions for the spherical bessel functions for large arguments:

$$|p_s|\underset{r\to\infty}{\longrightarrow}\frac{P_0}{k_3r}\left|\sum_{n=0}^{\infty}(2n+1)\sin\eta_n\exp(j\eta_n)P_n(\cos\theta)\right|. \quad (31)$$

III. EXPERIMENTAL APPARATUS

Measurements of the distribution-in-angle of sound scattered in water by metal cylinders were made for the purpose of checking the theory. These measurements were made in a large steel tank at or near a frequency of one megacycle per second. A sound projector in one end of the tank irradiated the scatterer with sound. A receiving hydrophone was mounted in such a way that it could easily be moved to any position lying on a circle concentric with the scatterer, and served to measure the distribution in angle of the pressure in the scattered wave. Short wave trains or "pulses" of sound were used in order that the measurement of each pulse could be effectively completed before sound reflected from the walls of the tank could reach the receiving hydrophone. A novel feature, frequency modulation of the pulse repetition rate, served to identify interfering pulses which, still reverberating in the tank from the previous transmitted pulse, happened to arrive at the receiver at the same time as the pulse to be measured. A small adjustment of the average pulse repetition rate was effective in controlling interference of this type. Both transducers employed x-cut quartz crystals operated at resonance. Serious distortion of the short (64 μsec) pulses by the transducers was prevented by lowering the Q of the quartz crystals by increasing the radiation loading. This was accomplished by inserting between the crystals and the water an acoustic quarter-wave transformer in the form of a thin disk of Plexiglas. The amplitude of the scattered sound pulses was measured by a modified substitution method, an oscilloscope being used as an indicator. The pulses were brought to a standard deflection on the oscilloscope, changes in the pulse amplitude being compensated by changes in the attenuation in the receiving system.

IV. COMPARISON OF THEORY AND EXPERIMENT

The experimental data were normalized so that they could be compared with scattering patterns computed from the theory. In order to do this, the amplitude of the pressure in the incident wave (P_0) was measured by moving the receiving transducer to the position of the

---

[8] See reference 3. Care must be taken to distinguish between the cylindrical and spherical cases, since the same symbols are used for the scattering phase-angles in both cases.

TABLE II. Values of $\zeta_n(x_1, \sigma)$ for the spherical case for $\sigma = \frac{1}{3}$.

	$n=0$	$n=1$	$n=2$	$n=3$	$n=4$	$n=5$	$n=6$	$n=7$	$n=8$	$n=9$
0	0.00°	−45.00°	0.00°	0.00°	0.00°	0.00°	0.00°	0.00°	0.00°	0.00°
2	1.16	−44.72	3.05	1.94	1.41	1.13	0.96	0.81	0.73	0.64
4	4.66	−43.57	12.77	7.77	5.91	4.66	3.91	3.33	2.93	2.62
6	10.58	−41.62	29.97	17.88	13.38	10.38	8.73	7.50	6.58	5.88
8	18.89	−38.54	51.40	31.55	23.47	18.83	15.93	13.58	12.19	11.01
0	29.12	−33.76	70.41	46.79	35.44	28.67	24.25	20.74	18.32	16.09
2	40.28	−26.18	83.89	60.52	47.88	39.29	33.22	29.67	25.84	23.32
4	51.05	−12.80	−86.94	71.44	58.67	50.00	43.23	38.34	34.49	31.51
6	60.55	+16.87	−80.31	79.64	67.68	59.02	52.20	46.57	42.41	38.72
8	68.41	89.15	−75.00	85.78	74.68	66.42	59.69	54.53	49.80	45.77
0	74.78	−25.58	−70.20	−89.46	80.14	72.50	66.17	60.82	56.28	52.29
2	79.92	+9.84	−65.27	−85.58	84.46	77.29	71.50	66.61	62.27	58.30
4	84.14	30.55	−59.50	−82.18	87.97	81.17	75.75	71.13	67.13	63.16
6	87.71	48.97	−52.57	−78.94	−89.07	84.39	79.27	74.89	71.11	67.61
8	−89.15	61.45	−41.61	−75.41	−86.44	87.06	82.18	78.10	74.62	71.07
0	−86.24	70.09	−25.03	−70.56	−83.95	89.38	84.63	80.80	77.41	74.43
	−83.36	76.48	−0.51	−55.48	−81.37	−88.53	86.75	83.03	79.87	77.00
4	−80.31	81.81	+27.37	−81.31	−78.27	−86.56	88.61	84.98	81.93	79.23
6	−76.72	88.64	49.05	−68.79	−73.44	−84.57	−89.70	86.69	83.75	81.23
8	−72.00	75.11	63.24	−59.85	−59.37	−82.35	−88.10	88.21	85.33	82.88
0	−64.84	85.64	72.99	−47.06	+65.07	−79.48	−86.50	89.61	86.71	84.30
2	−51.66	89.00	81.77	−24.13	−87.41	−74.70	−84.81	−89.07	87.99	85.62
4	−22.39	−88.45	−65.12	+13.38	−80.54	−60.64	−82.81	−87.76	89.17	86.81
6	+26.20	−86.12	+73.10	47.64	−75.60	+48.49	−80.07	−86.41	−89.71	87.88
8	56.58	−83.70	80.80	68.81	−70.16	84.65	−75.21	−84.90	−88.62	88.89
.0	70.03	−80.89	84.41	−88.10	−62.36	−88.16	−60.25	−83.03	−87.50	89.85

atterer. After normalization, it was still necessary to dd a factor amounting to 1.9 db to the amplitude of the attered sound in order to bring the experimental data nto good agreement with the theory. This correction ctor has been explained, and its value computed with ood accuracy, by taking into account the fact that the lumination of the scatterer varies in phase and amplide along its length.[9]

The part of Eq. (26) which was evaluated in comuting the patterns was

$$\tfrac{1}{2}\left|\sum_{n=0}^{\sigma}\epsilon_n \sin\eta_n \exp(j\eta_n)\cos n\theta\right|,$$

nd the corresponding numerical scale is shown on all e patterns used as illustrations. The values of Poisson's tio for the various scatterers were assumed, because the difficulty of measuring this constant directly; but the values of Young's modulus were measured (to within ±5 percent) by finding the frequency of the first mode of flexual vibration of the cylindrical specimen mounted so that it could vibrate as a fixed-free bar. The value of x_1 was then determined by means of Eq. (5). In some cases where the pattern was very sensitive to frequency, it was necessary to choose a value of x_1 slightly different from that based on the Young's modulus measurement in order to bring the measured and computed patterns into agreement. Comparison of the value of Young's modulus corresponding to the assumed value of x_1 with the measured value serves in these cases to indicate the degree of agreement between experiment and theory.

Figures 3 through 13 are measured and computed scattering patterns for cylinders of various sizes. The pressure in the scattered wave is plotted linearly against scattering angle. In each case the arrow indicates the direction of the incident sound. The angle θ is measured from the top center of the graph, the incident sound coming from the direction $\theta = 180°$. For each size of

---

[9] J. J. Faran, Jr., *Sound Scattering by Solid Cylinders and pheres*, Technical Memorandum No. 22 (March 15, 1951), coustics Research Laboratory, Harvard University, Cambridge, assachusetts.

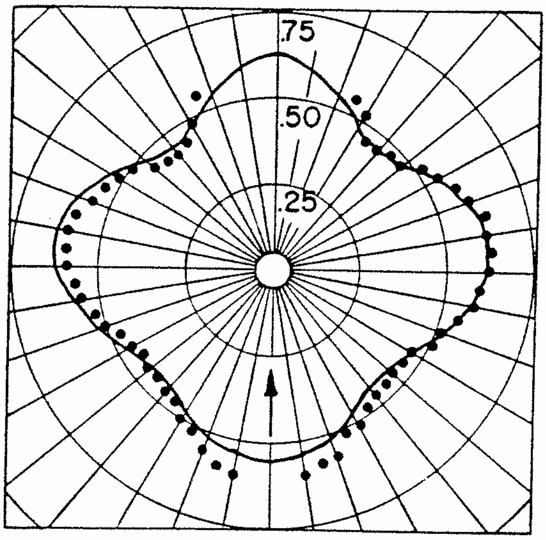

FIG. 3. Scattering pattern for brass cylinder 0.0322 in. in diameter at 1.00 mc/sec. *Points:* Measured amplitude of pressure in the scattered wave. The measured Young's modulus was 10.1 $\times 10^{11}$ dynes/cm^2. *Curve:* Computed pattern for $x_3=1.7$, $x_1=0.6$, $\sigma=\frac{1}{3}$, $\rho_1=8.5$ g/cm^3.

scatterer, the pattern computed on the basis that the scatterer is rigid and immovable is included for comparison.

Figures 3 and 4 show scattering patterns for brass and steel (drill rod) cylinders of the same size, for each of which $x_3=1.7$. These patterns are both very similar to that for a rigid, immovable scatterer of the same size (Fig. 5).

Figures 6–8 show scattering patterns for cylinders of various materials twice as large in diameter, that is, $x_3=3.4$. The pattern for a brass cylinder of this size (Fig. 6) is somewhat unusual; the amplitude of sound scattered back in the direction of the source is nearly zero. This near-null in the back-scattered sound is fully explained by the mathematical solution in which the

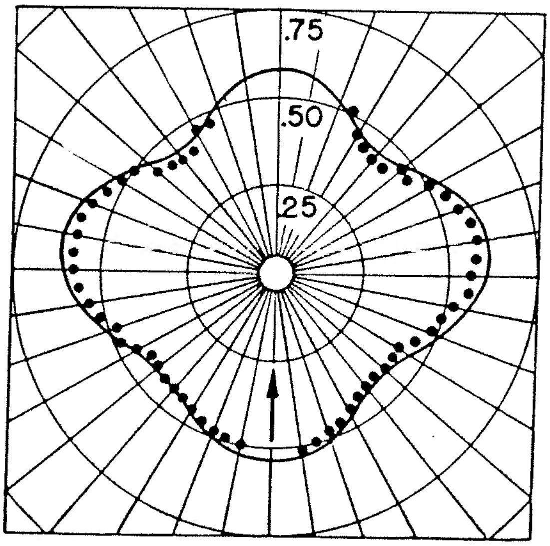

FIG. 4. Scattering pattern for steel cylinder 0.032 in. in diameter at 1.00 mc/sec. *Points:* Measured amplitude of pressure in the scattered wave. The measured Young's modulus was 20.0×10^{11} dynes/cm^2. *Curve:* Computed pattern for $x_3=1.7$, $x_1=0.45$, $\sigma=0.28$, $\rho_1=7.7$ g/cm^3.

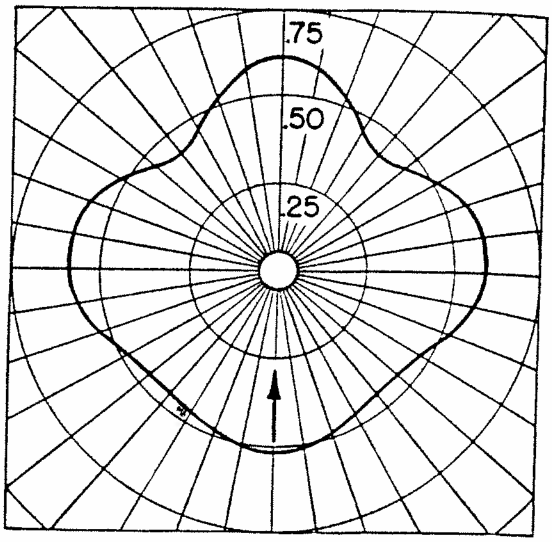

FIG. 5. Computed amplitude of pressure in wave scattered by a rigid, immovable cylinder for $x_3=1.7$.

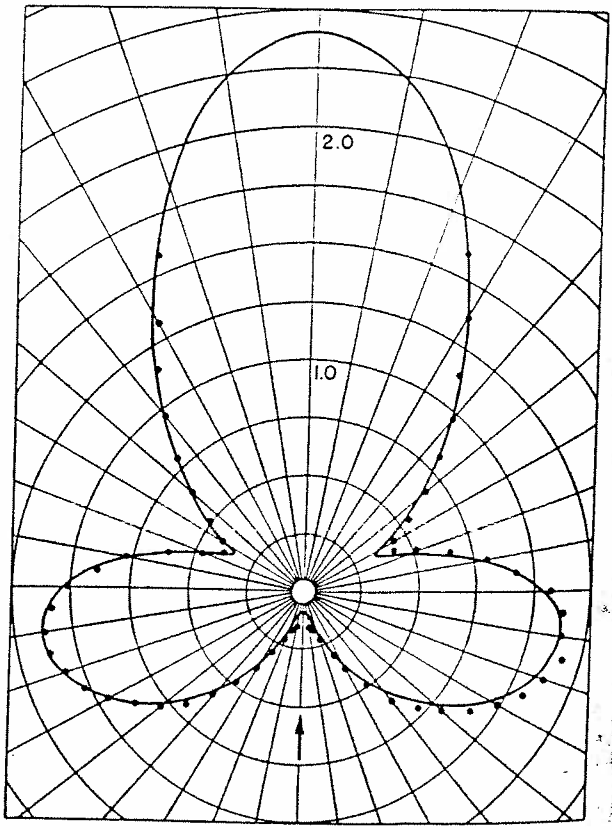

FIG. 6. Scattering pattern for brass cylinder 0.0625 in. in diameter at 1.02 mc/sec. *Points:* Measured amplitude of pressure in the scattered wave. The measured Young's modulus was 10.4×10^{11} dynes/cm^2. *Curve:* Computed pattern for $x_3=3.4$, $x_1=1.185$, $\sigma=\frac{1}{3}$, $\rho_1=8.5$ g/cm^3 (corresponding to $E=10.5\times 10^{11}$ dynes/cm^2).

rm for $n=2$ in the series for the scattering pattern ıddenly becomes very large in amplitude and of the roper phase to cancel the sum of all the other terms at $=180°$. This, in turn, is brought about by the presence an infinity in the $\tan\zeta_n(x_1, \sigma)$ function for $\sigma=\frac{1}{3}$ at $_1=1.18\cdots$ (corresponding to a normal mode or resonance of the scatterer), in the neighborhood of which this ınction goes rapidly through a wide range of values ausing the variations in the coefficient of the $n=2$ erm. The value of x_1 for the computed pattern of ig. 6 was chosen to give a deep notch at $\theta=180°$, and he frequency at which the experimental pattern was

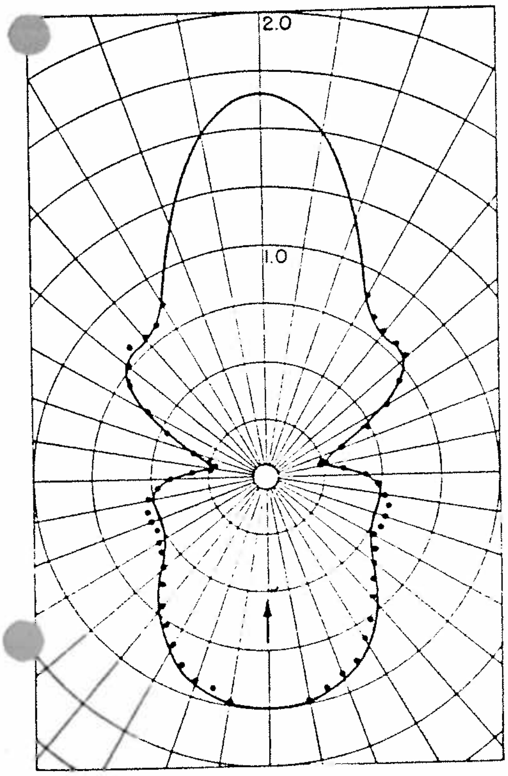

FIG. 7. Scattering pattern for copper cylinder 0.0625 in. in diameter at 1.00 mc/sec. *Points:* Measured amplitude of pressure in the scattered wave. The measured Young's modulus was 11.9×10^{11} dynes/cm². *Curve:* Computed pattern for $x_3=3.4$, $x_1=1.08$, $\sigma=\frac{1}{3}$, $\rho_1=8.9$ g/cm³ (corresponding to $E=12.7\times10^{11}$ dynes/cm²).

measured was chosen the same way. Figure 7 is the scattering pattern for a copper cylinder of the same size. The value of x_1 for the copper cylinder is near enough to 1.18 that the coefficient of the $n=2$ term is still large, but in this case it is of the opposite phase and causes the sound scattered in the direction $\theta=180°$ to be somewhat larger in amplitude than that scattered by a rigid, immovable cylinder of this size (Fig. 9). The velocity of sound in steel is so much higher than that in brass or copper that this scatterer behaves nearly as though it were rigid and immovable, and its scattering pattern (Fig. 8) is little different from that for the rigid, immovable case.

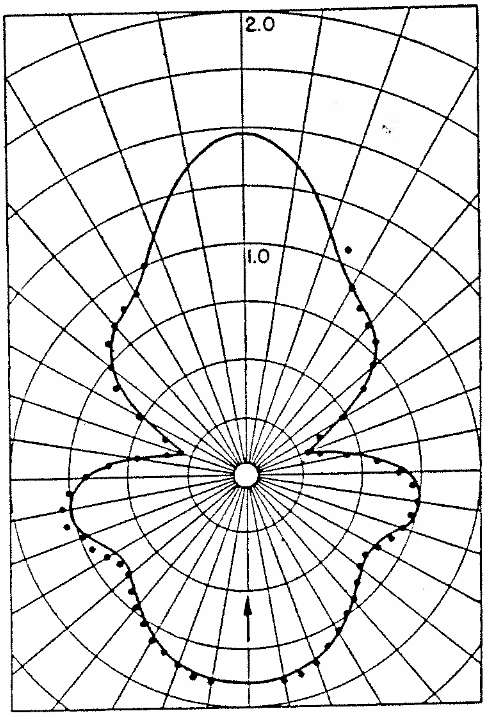

FIG. 8. Scattering pattern for steel cylinder 0.0625 in. in diameter at 1.00 mc/sec. *Points:* Measured amplitude of pressure in the scattered wave. The measured Young's modulus was 19.5×10^{11} dynes/cm². *Curve:* Computed pattern for $x_3=3.4$, $x_1=0.9$, $\sigma=0.28$, $\rho_1=7.7$ g/cm³.

Figures 10, 11, and 12 are scattering patterns for brass, steel, and aluminum cylinders for which $x_3=5.0$.

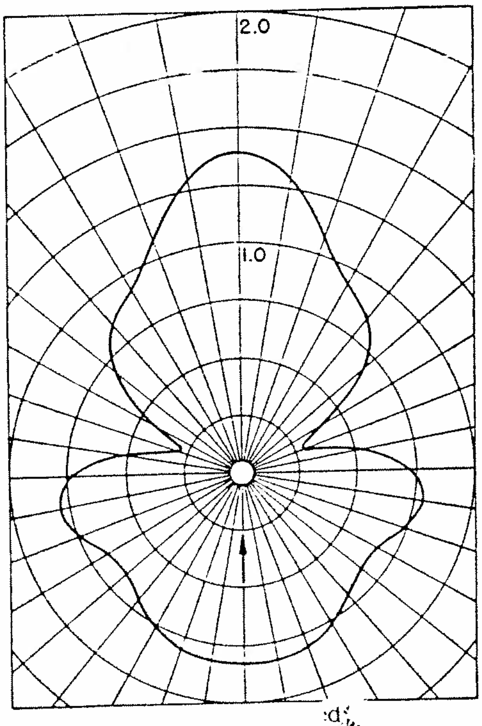

FIG. 9. Computed amplitude of pressure [illegible]ave scattered by a rigid, immovable cylinder for $x_3=3.4$.

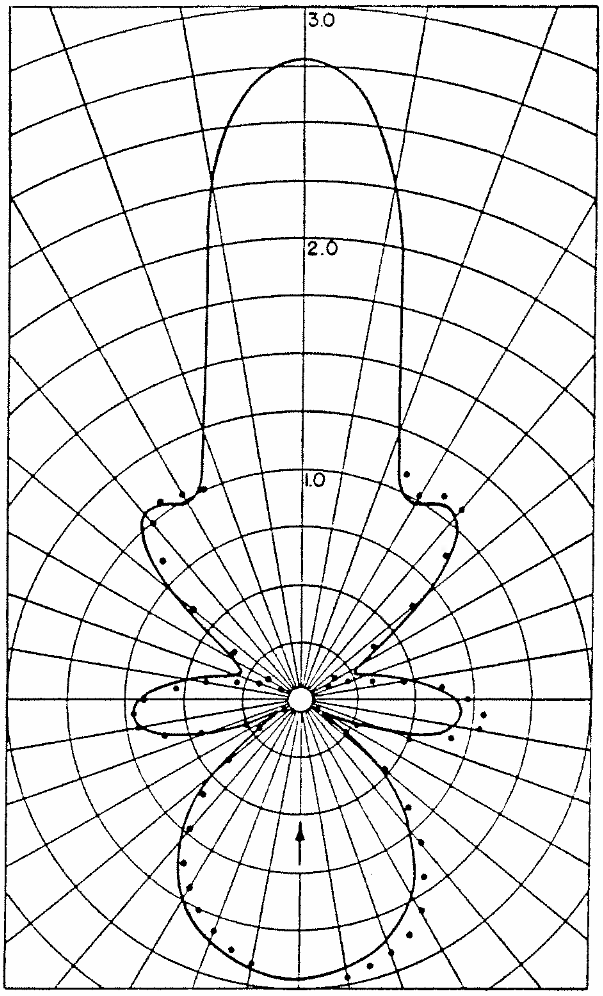

FIG. 10. Scattering pattern for brass cylinder 0.093 in. in diameter at 1.015 mc/sec. *Points:* Measured amplitude of pressure in the scattered wave. The measured Young's modulus was 10.0×10^{11} dynes/cm^2. *Curve:* Computed pattern for $x_3=5.0$, $x_1=1.78$, $\sigma=\frac{1}{3}$, $\rho_1=8.5$ g/cm^3 (corresponding to $E=10.2\times10^{11}$ dynes/cm^2).

The frequency of measurement of the pattern of the brass scatterer was chosen to give the deepest notch at 120°, and the value of x_1 was chosen to make the patterns agree. The choice of the value of x_1 is well substantiated by the measurement of the Young's modulus of this scatterer, since the value of E corresponding to the chosen value of x_1 is within 2 percent of the measured value. Figure 11 shows that, just as in the case of brass (Fig. 4), there is a near-null in the sound back-scattered from a steel cylinder at a frequency near that of the lowest-frequency normal mode which, for $\sigma=0.28$, occurs at $x_1=1.30\cdots$. Figure 12 shows that the same is true of an aluminum scatterer of the same size. Although the velocity of compressional waves in steel is not the same as that in aluminum, the values of Poisson's ratio differ sufficiently that this normal mode occurs in these two materials for the same physical size of the scatterers. These two patterns are so similar that they are seen to depend much more critically upon the value of x_1 than upon the density of the scatterer. The pattern for a rigid, immovable cylinder of the same size is shown in Fig. 13, and it is apparent that all these patterns for metal cylinders of this size bear little resemblance to this limiting case.

The theory thus verifies the existence of nulls in the back-scattered sound for cylinders of various metals, and at the proper frequencies; but a further test is to see whether it predicts properly the manner in which the amplitude of the back-scattered sound (and the shape of the entire pattern) changes with frequency. In order to test this, patterns were measured for the brass cylinder of Fig. 6 and the steel cylinder of Fig. 11 at two other frequencies, 3 percent below and above that at which the reference patterns were measured. The corresponding patterns predicted by the theory were computed by making a corresponding change in the values of the x parameters. In Fig. 14, the pattern of Fig. 6 is reproduced in the center, and those for 3 percent changes in frequency are shown at either side. In Fig. 15, the pattern of Fig. 11 is reproduced in the center, and the patterns for 3 percent changes in frequency are shown on either side. The theory is seen to predict the changes in the measured patterns with gratifying precision. These groups of patterns also emphasize the fact that the null

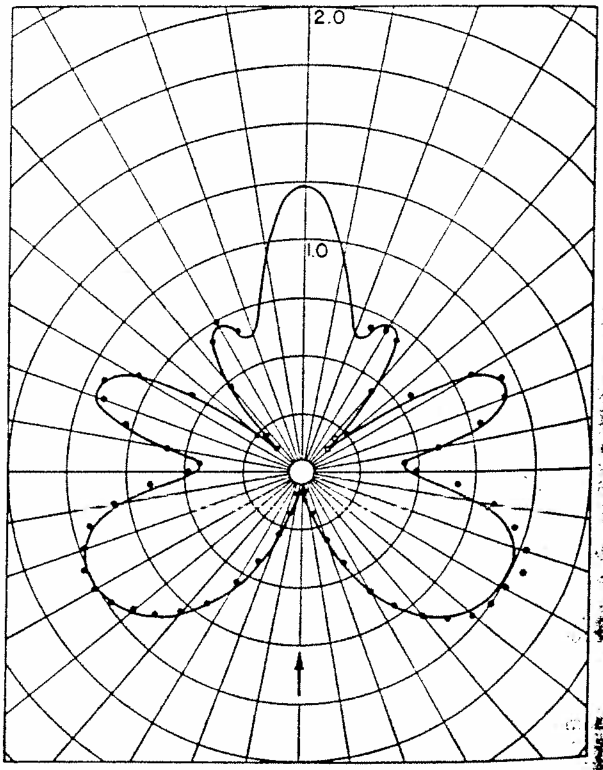

FIG. 11. Scattering pattern for steel cylinder 0.09375 in. in diameter at 0.99 mc/sec. *Points:* Measured amplitude of pressure in the scattered wave. The measured Young's modulus was 19.3×10^{11} dynes/cm^2. *Curve:* Computed pattern for $x_3=5.0$, $x_1=1.293$, $\sigma=0.28$, $\rho_1=7.7$ g/cm^3 (corresponding to $E=19.7\times10^{11}$ dynes/cm^2).

the back-scattered sound is very sensitive to quency.

Measurements of scattering by a few spheres were ıde with this apparatus. However, because the sound ıttered by a sphere diverges in three dimensions ıstead of two, as in the case of a long cylinder), the ɜasurement was found to be very difficult, because of e reduced margin of signal to noise. The measureents (and also computations) indicate that, although pid changes in the pattern do occur, there is no null in e so[illegible] back-scattered in water by a brass sphere, ɜar its lowest-frequency normal mode of vibration.

V. REMARKS ON THE BEHAVIOR OF SOLID SCATTERERS

It is interesting to examine the behavior of certain of ıe functions which appear in the mathematical soluon, especially the $\tan\zeta_n(x_1, \sigma)$ functions. As noted ›ove, it can be shown that the infinities of the ınζ$_n(x_1, \sigma)$ functions occur at precisely the frequencies f those normal modes of free vibration of the scattering ody which satisfy the conditions of symmetry of the :attering problem. This can be done by applying oundary conditions to expressions for displacement and ilatation written in general form in terms of an unnown frequency. The boundary conditions, for free ibrations, are simply that the normal component of tress and the tangential components of shearing stress at the surface of the body must both vanish. Solving the resultant equation for frequency (in terms of unknown x_1 and x_2 parameters) gives a condition which, in the cylindrical case, is identical to requiring the denominator of Eq. (24) to vanish.[10] For $\sigma=\frac{1}{3}$, the first few of these normal modes occur at the following values of the frequency parameter:

for $n=0$, $x_1=2.17\cdots$, $5.43\cdots$, $8.60\cdots$;
for $n=1$, $x_1=1.43\cdots$, $3.27\cdots$, $3.74\cdots$;
for $n=2$, $x_1=1.18\cdots$, $2.25\cdots$, $3.98\cdots$;
for $n=3$, $x_1=1.81\cdots$, $3.01\cdots$, $4.65\cdots$;
for $n=4$, $x_1=2.36\cdots$, etc.

The first normal modes for $n=1$, 2, and 3 occur for lower values of x_1 (lower frequencies) than that for $n=0$, contrary to what we might expect. The reason for this is that there are no shear waves associated with the $n=0$ normal modes. The complicated wave structure which comprises a normal mode can be realized at a much lower frequency with shear waves than without, because the velocity of shear waves is so much lower than that of compressional waves.

[illegible] functions $\tan\zeta_n(x_1, \sigma)$ in

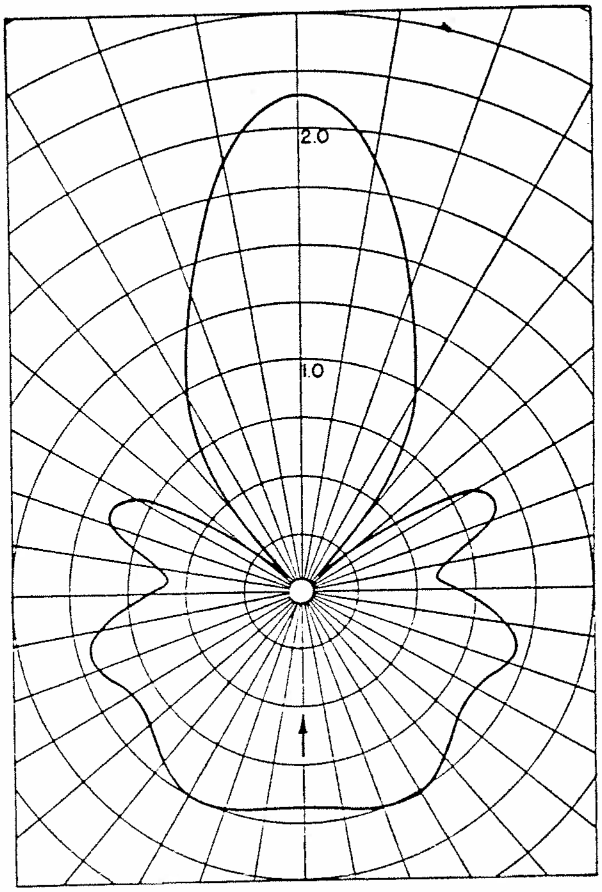

FIG. 13. Computed amplitude of pressure in wave scattered by a rigid, immovable cylinder for $x_3=5.0$.

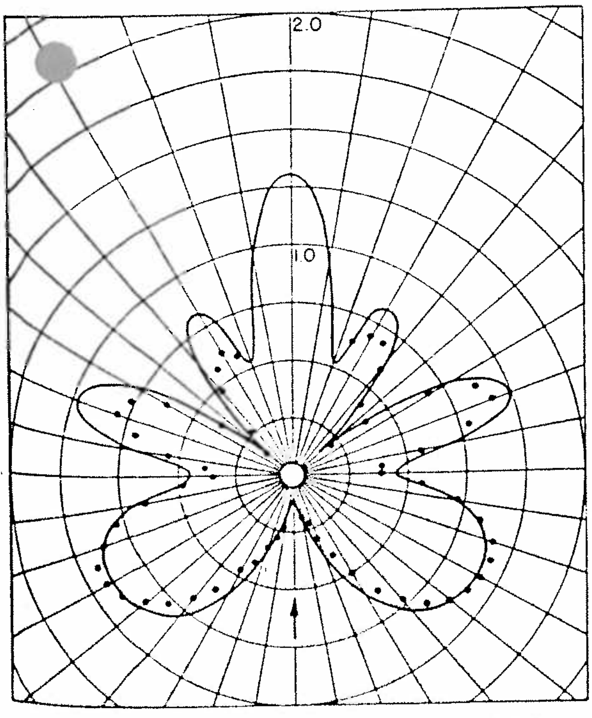

FIG. 12. Scattering pattern for aluminum cylinder 0.0925 in. in di[illegible]

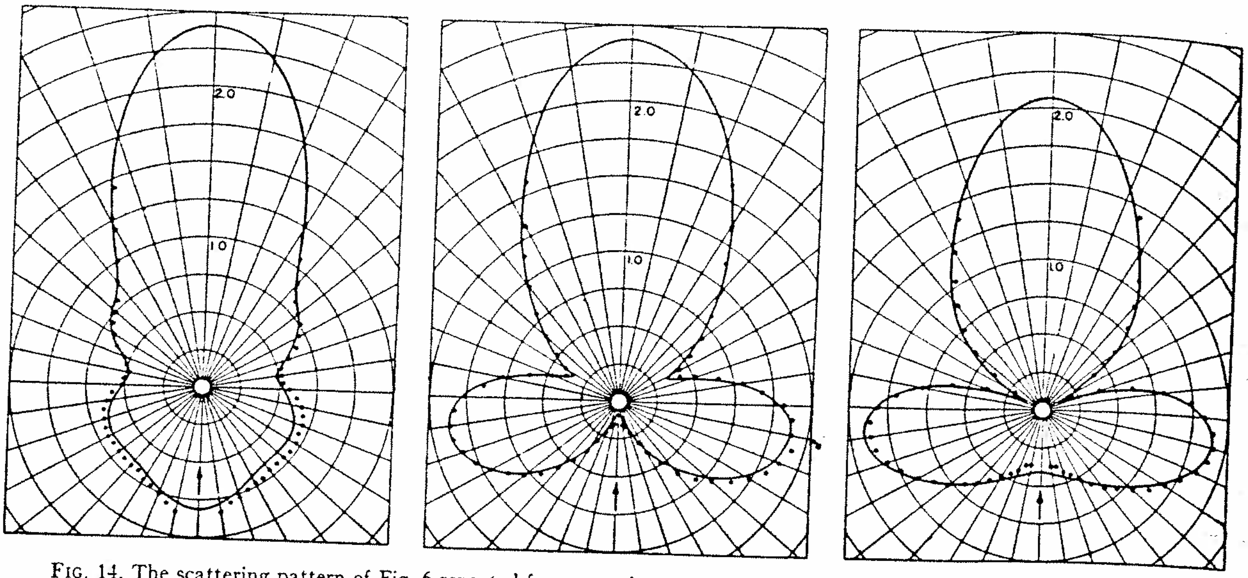

FIG. 14. The scattering pattern of Fig. 6 repeated for comparison with measured and computed patterns for frequencies 3 percent higher (right) and 3 percent lower (left).

$\tan\alpha_n(x_1)$. It is interesting to note that the infinities of these functions also correspond to frequencies of normal modes of free vibration of the (fluid) scatterer, since the infinities of $\tan\alpha_n(x_1)$ occur at the zeros of $J_n(x_1)$ or $j_n(x_1)$, in the cylindrical and spherical cases, respectively.

The coefficient c_n in the series for the scattering pattern does not attain its maximum value at exactly the frequencies of the normal modes of free vibration of the scatterer. Since the amplitude of c_n is proportional to $\sin\eta_n$, c_n reaches its maximum value when $\tan\eta_n$ becomes infinite. This represents a shift in the resonant frequency of the normal mode, and this shift is attributed to the reactive component of the acoustic impedance presented to the scatterer by the surrounding fluid, i.e., the reactive component of the radiation loading. In the case of solids having densities greater than that of the surrounding fluid, however, this frequency shift is usually small.

While measurements were being made with the experimental apparatus at frequencies near that of a normal mode, it was in some cases possible to observe "ringing" of that normal mode following the end of the pulse; that is, long transients could be observed at the end (and at the beginning) of the scattered pulse. By adjusting the frequency to give the maximum amplitude of the transient at the end of the pulse, it was thus possible to measure the frequencies of various normal modes. It was also possible to identify the order n of the excited mode, because the amplitude of the transient following the pulse was proportional to $\cos n\theta$. These transients were not noticeable in the case of the first normal mode for $n=2$. Apparently the damping by

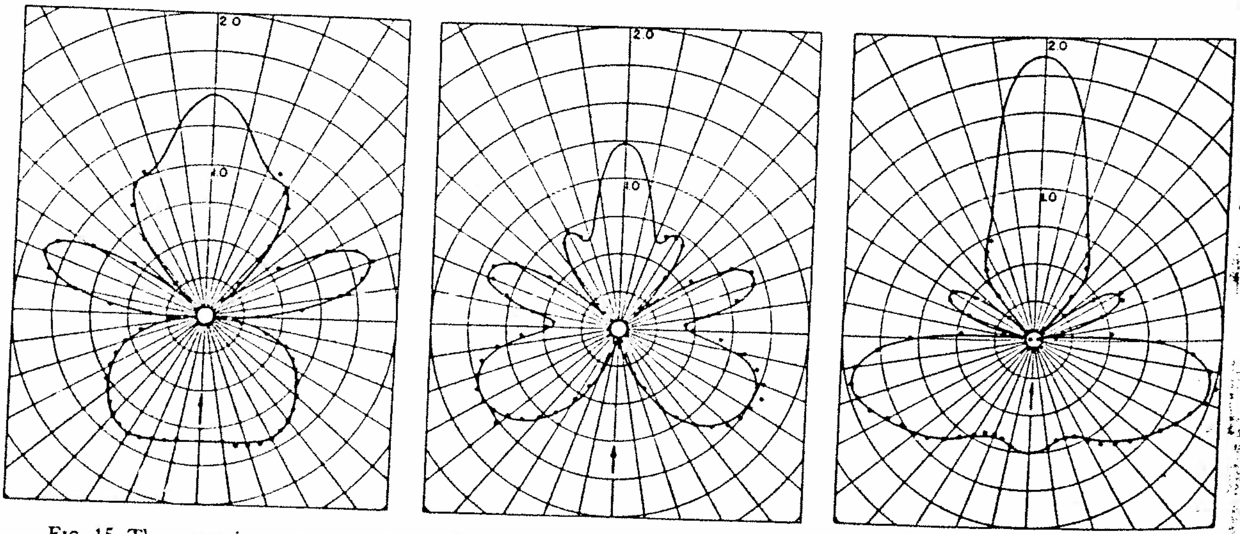

FIG. 15. The scattering pattern of Fig. 11 repeated for comparison with measured and computed patterns for frequencies 3 percent higher (right) and 3 percent lower (left).

ation into the water was great enough to cause any ;ing to die out quickly. However, the first normal les for $n=0$, 1, and 3 were observed and identified brass and steel cylindrical scatterers of appropriate s and showed good agreement with the frequencies dicted by the theory.

'hat there are sizeable shifts in the frequencies of the mal modes with changes in Poisson's ratio suggests t finding the frequencies of one or more of these mal modes of vibration might provide a method of asuring Poisson's ratio for cylindrical or spherical cimens. The variation of the frequencies of these mal modes with Poisson's ratio is illustrated in s. 16 and 17, where the values of x_1 at which the first mal modes for $n=0$, 1, 2, 3, and 4 occur are plotted functions of Poisson's ratio. The variation of the ond normal mode for $n=2$ is also shown in the graph the spherical case. In this connection, as well as in scattering problem itself, the potential utility of ving the $\zeta_n(x_1, \sigma)$ functions computed for a wide ge of values of Poisson's ratio will be evident. A nputation program to yield these results appears to justified. The frequencies of the normal modes cannot computed explicitly, but can be found easily from the ations of the infinities of the $\tan\zeta_n(x_1, \sigma)$ functions.

It is interesting to compare the behavior of the $\tan\Phi_n$ ictions for solid and fluid scatterers as x_1, the frequency parameter for the scatterer, approaches zero. r solid scatterers, either cylindrical or spherical, as $\to 0$,

$$\tan\Phi_n\to 0, \quad n\neq 1; \quad \tan\Phi_1\to\rho_3/\rho_1;$$

ile for fluid scatterers, where

$$\tan\Phi_n=(-\rho_3/\rho_1)\tan\alpha_n(x_1),$$

$x_1\to 0$,

$$\tan\Phi_n\to(\rho_3/\rho_1)n.$$

neither case, by letting $x_1\to 0$, do we realize the case the rigid, immovable scatterer where $\tan\Phi_n=0$ for all In order that $x_1=\omega a/c_1\to 0$ at finite frequencies in the id case, the velocities of both the compressional and ear waves must become infinite, and the scatterer does leed become rigid. The only term where $\tan\Phi_n$ does t vanish is that for $n=1$. This deviation from the id, immovable case is simply due to oscillation of the itterer as a whole in synchronism with the incident and field. Thus, by setting $x_1=0$ in the solution given re for solid scatterers, we can calculate the scattering m a rigid, *movable* cylinder or sphere of density ρ_1. To ss to the case of the rigid, immovable scatterer, we ist also require that the density of the scatterer become infinite. In the case of a fluid scatterer, as $x_1\to 0$, ly $\tan\Phi_0$ approaches the value for the limiting case of igid, immovable scatterer. For $n=1$, $\tan\Phi_n$ behaves the same way as in the case of the solid scatterer, and presents oscillation of the scatterer in synchronism th the incident sound. Now, for fluid scatterers, in the fluid become incompressible; but as this happens, the scatterer does not necessarily become rigid to shear distortions. It must then be that, for $n=2$ and higher, shape distortions of the incompressible fluid scatterer make the components of the scattered wave different from what they would be if the scatterer were rigid. Because the fluid scatterer never becomes rigid as $x_1\to 0$, one can only pass from this solution to the case of the rigid, immovable scatterer by letting the density become infinite.

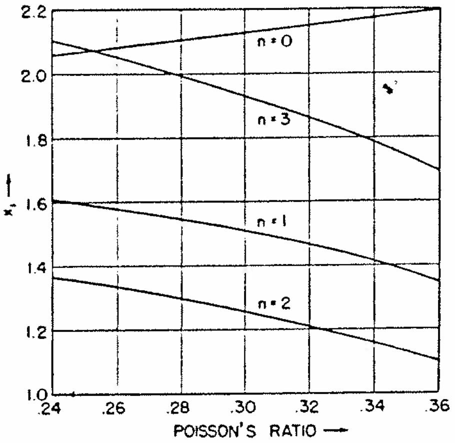

FIG. 16. The values of x_1 for the first few symmetrical normal modes of free vibration of a solid cylinder plotted as functions of Poisson's ratio.

Two summary comments can be added regarding the general features of scattering by solid cylinders and spheres. If the frequency of the incident sound is lower than that of the first symmetrical normal mode of free vibration of the solid scatterer, and if the density of the scatterer is greater than that of the liquid, there is little difference between the scattering pattern for the solid scatterer and that for a rigid, immovable scatterer. But, rapid changes in the shape of the scattering pattern and in the total scattered power (or scattering cross section)

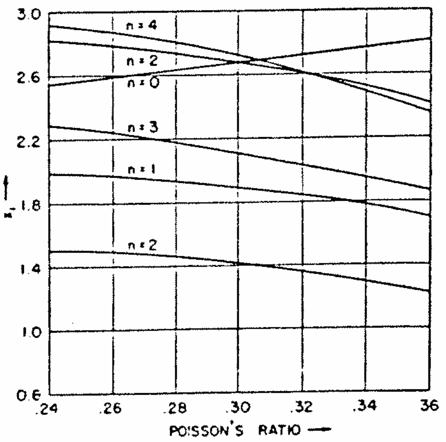

FIG. 17. The values of x_1 for the first few symmetrical normal modes of free vibration of a solid sphere plotted as functions of

can occur with small changes in frequency in the vicinity of certain of the normal modes of free vibration of the solid scatterer. These changes include the appearance of deep minima in the scattering pattern at certain angles and may include, for cylinders, a near-null in the sound scattered back toward the source.

VI. ACKNOWLEDGMENTS

The author is indebted to Professor F. V. Hunt for guidance and encouragement throughout this invest tion. The assistance of Dorothea Greene, who formed the laborious computations for Figs. 16 and is gratefully acknowledged.

THE JOURNAL OF THE ACOUSTICAL SOCIETY OF AMERICA VOLUME 23, NUMBER 4 JULY, 1

The Growth of Subharmonic Oscillations

W. J. Cunningham
Yale University, New Haven, Connecticut

(Received January 14, 1951)

Subharmonic oscillations at one-half the frequency of excitation may appear in certain types of oscillating systems, among which is the direct-radiator loudspeaker. These oscillations occur at very nearly the resonant frequency of the system when the parameters of the system are made to vary at twice this frequency. The rate of growth of the subharmonic depends upon the amount of variation of the parameters relative to the dissipation in the system. If the dissipation is small, the rate of growth may be large. In the loudspeaker, conditions are such that the rate of growth is usually small for typical conditions of operation.

THE generation of subharmonic oscillations by a direct-radiator loudspeaker has often been observed.[1–4] Such oscillations usually occur at one-half the frequency of the current supplied to the loudspeaker, and appear for only certain discrete frequencies near the center of the audio spectrum. In most cases, the subharmonic is not present unless the loudspeaker is being operated near its maximum power. When present, the subharmonic is easily audible, even though sound pressure measurements indicate the amplitude of the subharmonic is only a few percent relative to the fundamental. The statement has been made that this subharmonic distortion is usually of little practical importance in the operation of the loudspeaker.[5] The reasoning is based on the observed fact that an appreciable length of time is required for the amplitude of the subharmonic to grow to its ultimate value. Since typical program material is of constantly changing nature, there is little opportunity for the subharmonic to build up. In the following rather simple discussion, the growth of the subharmonic oscillation is considered with the intent of determining what factors influence the rate of growth and why this rate is low for the loudspeaker.

Subharmonic oscillation at one-half the frequency of an exciting force may occur in oscillating systems having a single degree of freedom.[6,7] For the subharmonic to appear, the quiescent resonant frequency of the system must be very nearly one-half the exciting frequency. Further, operation must be such that under excitation the resonant frequency of the system is caused to vary at the exciting frequency. This variation must take place in such a way that sufficient energy is being supplied to the system to replace that lost by dissipation. If more than this amount of energy is supplied, the amplitude of the subharmonic grows, in theory, without limit. Ultimately, in practical systems, some additional effect takes over and the amplitude achieves a steady value.

In order to give a simple example of this type of operation, an electric circuit will be considered in some detail. This circuit contains in series combination an inductance L, a resistance R, and a capacitance C. If q is the instantaneous charge on the capacitance, the sum of voltages around the circuit is

$$L\ddot{q}+R\dot{q}+q/C=0, \tag{1}$$

where dots indicate time derivatives. In some way the capacitance is made to vary sinusoidally in time by an amount ΔC about the mean value C_0. The instantaneous capacitance is

$$C=C_0(1+a\sin 2\omega_1 t), \tag{2}$$

where the angular frequency of the variation is taken as $2\omega_1$, and $a\equiv\Delta C/C_0$. Evidently a can never exceed unity. It is possible to show that such a variation in capacitance can add energy to the oscillating circuit. The resonant angular frequency of the circuit in its quiescent

---

[1] H. F. Olson, *Acoustical Engineering* (D. Van Nostrand Company, Inc., New York, 1947), p. 167.

[2] P. O. Pederson, J. Acoust. Soc. Am. 6, 227–238 (1935), and 7, 64–70 (1935).

[3] F. von Schmoller, Telefunken Zeitung 67, 47–54 (June, 1934).

[4] G. Schaffstein, Hochfrequenztechn. Elektroakust. 45, 204–213 (1935).

[5] See reference 2. Also, H. S. Knowles, "Loudspeakers and room acoustics," Sec. 22, *Henney's Radio Engineering Handbook* (McGraw-Hill Book Company, Inc., New York, 1941), p. 902.

[6] N. Minorsky, *Nonlinear Mechanics* (Edwards Brothers, Inc., Ann Arbor, 1947), Chap. XIX.

[7] N. W. McLachlan, *Ordinary Nonlinear Differential Equations* (Oxford University Press, London, 1950), Chap. VII.

Some applications of scattering.

* Catfish farming !

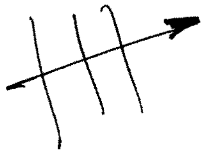

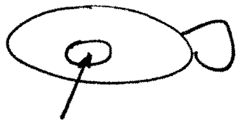

swimbladder (air bubble)
very effective scatterer.

* Flaw detection in NDE

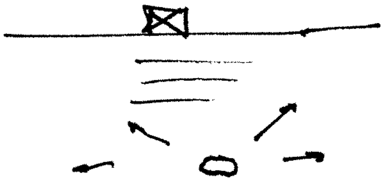

* Dynamic properties of viscoelastic materials containing inclusions

used to absorb sound.

Shear modulus is much more lossy than the bulk modulus

→ desirable to convert bulk waves into shear waves.

→ introduce inhomogeneities (inclusions).

conversion into some shear motion

↓

increased losses
(dissipation into heat)

usually $ka \ll 1$ (Rayleigh scattering)

2. Kerner model

Proc. Phys. Soc. London 69, 808 - 513 (1956)

simple model:

- * assumes quasi-static ($ka \ll 1$)
- * and low volume fraction ϕ (no multiple scattering)

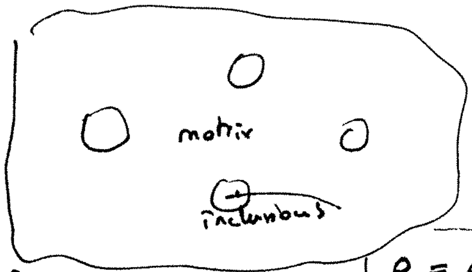

field around a scatterer is dominated by incident + scattered wave from that scatterer (not from surrounding scatterers)

air inclusions

$$\boxed{\rho = \rho_0(1-\phi) + \phi\rho_I}$$

$$: \frac{\rho_0-\rho}{\rho_0-\cancel{\rho_I}} \approx \rightarrow \quad \phi = 1 - \frac{\rho}{\rho_0}$$

; ρ = density of composite
ρ_0 = density of matrix only.

Then:

Bulk modulus
$$K = \frac{K_0(1-\phi)}{1+\frac{3\phi K_0}{4G_0}} \approx \frac{4(1-\phi)G_0}{3\phi} \quad (*)$$

Shear modulus
$$G = \frac{G_0}{1+\frac{5}{3}\phi}$$

K_0, G_0 : moduli of matrix
K, G : moduli of composite.

(G_0 complex!)

$|K_0| \gg |G_0|$ for viscoelastic materials $\Rightarrow \mathrm{Im}(K) = \mathrm{Im}(G_0)$

Good!

Indeed, attenuation is directly related to imaginary parts of moduli.

Bulk wave speed $c_B = \sqrt{\frac{K}{\rho}}$ complex $\Rightarrow$ k_B complex $\Rightarrow$ atten

Dilatational (longitudinal) wave speed $c_L = \sqrt{\frac{K + \frac{4}{3}G}{\rho}} \rightarrow \dots$

Shear wave speed $c_s = \sqrt{\frac{G}{\rho}} \Rightarrow \dots$

3. Norris Model

(Int. J. Eng. Science, Vol 24, 1986. 1271-1282)

General approach:

$$k_L^2 = k_{L0}^2 + \overbrace{\frac{4\pi n}{k_{L0}} A_c^c(0)}^{\text{complex.}}$$

perturbations due to scattering effects.

$$k_s^2 = k_{s0}^2 + \frac{4\pi n}{k_{s0}} A_s^s(0)$$

k_L, k_s = Long. and shear wavenumbers in effective material

k_{L0}, k_{s0} = " " " " in matrix only

n = number of scatterers per unit volume

$A_c^c(0)$, $A_s^s(0)$: Forward scattering coefficients for incident longitudinal and shear waves.

Assumptions:
- Quasi-static (low ka)
- low void fraction (no multiple scattering)
- (only 2 phases)

4. Bair-Kerr-Townend model

Coated inclusions: 3 phases.

Matrix
coating
inclusion.

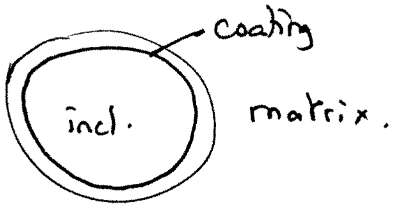

Ref. JASA 105 (3) 1999. (1527-1538)

Approach: GU-method. [Gaunaurd - Überall,
ref. JASA 71, 282-295 (1982)]

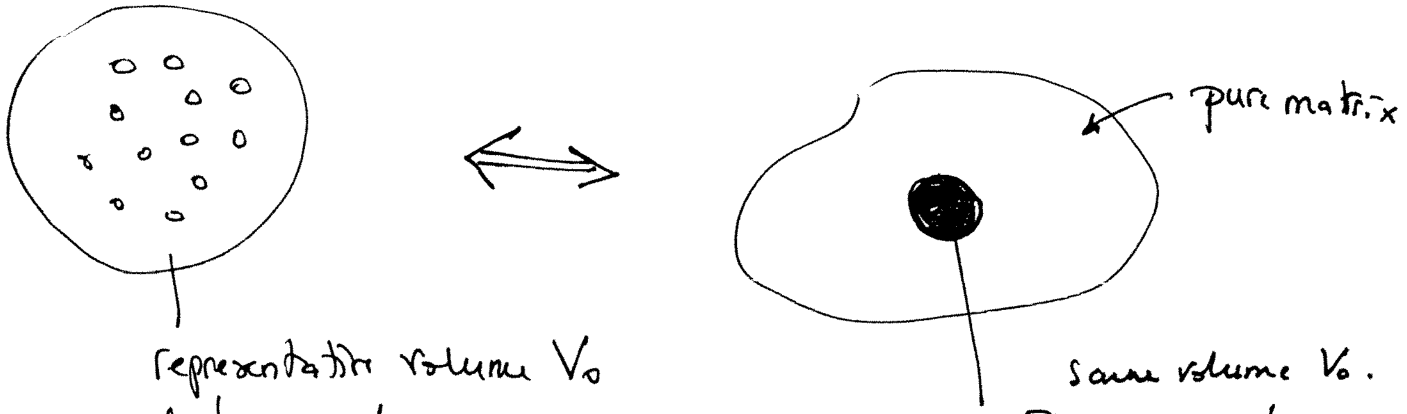

representative volume V_0
containing N inclusions
(representative of the effective material)

Same volume V_0.
Single scatterer
w/ effective material
properties.

(*) modeling: (see back.)

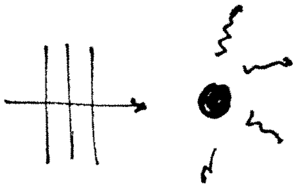

Scattered field described by
Scattering coefficient A^*_n
(ignores multiple scattering)

$*$: effective material.
n = n-order $\left(\sum_{n=0}^{\infty}\right)$.

Effective Medium Theory (EMT)

Key: $\boxed{A_n^* = \phi A_n}$

ϕ = void fraction

⇒ where A_n found from single inclusion problem.

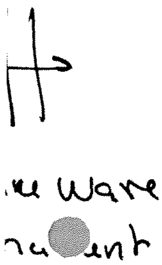

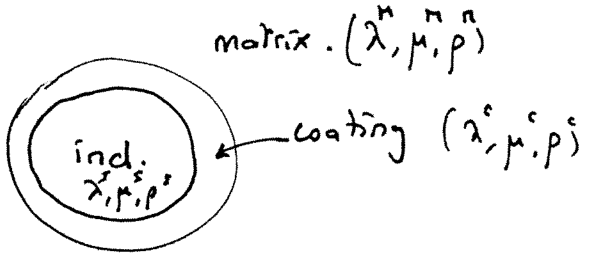

$\left\{\begin{matrix}\text{shear} \\ \text{compressional}\end{matrix}\right\}$ waves in coating and inclusi

to solve for A_n:

- express all fields in spherical harmonics
- Apply BC: continuity of normal stress ~~&~~ displacement @ boundari
- obtain a system of 8 equations, 8 unknowns.
- assume low ka → expand Bessel, Neuma, hankel
- retain only lowest order in ka ⇒ $n = 0, 1, 2$

$\underbrace{\text{monopoles}, \quad \text{dipoles}, \quad \text{quadrupoles}}$.

$A_0 \qquad A_1 \qquad A_2$